MIXING ZONE STUDIES OF THE WASTE WATER DISCHARGE FROM THE CONSOLIDATED PAPER COMPANY INTO THE WISCONSIN RIVER AT WISCONSIN RAPIDS, WISCONSIN

John A. Hoopes, Professor
Dong-Shan Wu, Research Assistant
Ramesh Ganatra, Research Assistant

March 1973

MIXING ZONE STUDIES OF THE WASTE WATER DISCHARGE FROM THE CONSOLIDATED PAPER COMPANY INTO THE WISCONSIN RIVER AT WISCONSIN RAPIDS, WISCONSIN

REPORT OF 1969 SUMMER FIELD SURVEYS

to the

Division of Environmental Protection
Department of Natural Resources
State of Wisconsin
and
Office of University Affairs
National Aeronautics and Space Administration

by

John A. Hoopes, Professor
Dong-Shan Wu, Research Assistant
Ramesh Ganatra, Research Assistant

Department of Civil and Environmental Engineering
University of Wisconsin

March 1973

ABSTRACT

A field survey of the effluent concentration distributions from the waste water discharge of the Kraft Division Mill, Consolidated Paper Company, into the Wisconsin River at Wisconsin Rapids, Wisconsin, was undertaken on September 12, 1969. Effluent concentrations were determined from measurements of the temperature distribution, using temperature as a tracer. Measurements of the velocity distribution in the vicinity of the outfall were also made. From the measurements horizontal and vertical concentration patterns of the waste discharge are developed. These patterns are analyzed and compared with the results of laboratory experiments and of several mathematical models to determine the macroscopic characteristics and relations governing the effluent spreading and dilution for the effluent and river conditions during the survey. These characteristics include the centerline concentration variation, the centerline trajectory and the lateral and vertical spreads of the effluent discharge. Due to limitations in the extent of the field observations, the analysis and comparison of the measurements is limited to the region within about 300 feet from the outfall. Effects of outfall submergence, of buoyancy and momentum of the effluent and of the pattern and magnitude of river currents on these characteristics are considered. Finally, using the field observations, with results from the laboratory experiments and mathematical models, the extent and shape of the mixing zone is estimated for the effluent and river conditions on September 12, 1969.

ACKNOWLEDGEMENTS

This investigation was sponsored by the Department of Natural Resources (DNR) of the State of Wisconsin and the Office of University Affairs of the National Aeronautics and Space Administration (NASA). This work is part of the research project entitled "Definition of the Mixing Zone for Waste Effluents Discharged into Surface Waters". Mr. Carroll Besadny, Mr. Everett Cann, Mr. Jerome McKersie and Mr. Francis Schraufnagel of the Environmental Protection Division of DNR and Professor James L. Clapp, principal investigator of the University of Wisconsin's Remote Sensing Grant from NASA, have provided continuing support and encouragement through the course of this work. The field survey was carried out with the cooperation and support of the Consolidated Paper Company. The operating personnel at the Kraft Division Mill in Wisconsin Rapids provided access to the plant facilities and information regarding plane operations without which the field surveys could not have been undertaken. The Engineering Experiment Station and the Environmental Monitoring and Data Acquisition Group (Institute of Environmental Studies) of the University of Wisconsin provided administrative support for this study.

The authors are indebted to student helpers Stanley D'Souza, Terry Johnson, Ming-Chung King and John Villemonte who provided able assistance in the field work and in the data reduction. Professors James Villemonte and Willard Murray (Visiting Assistant Professor), Civil and Environmental Engineering

Department at the University of Wisconsin, reviewed and gave many helpful suggestions on this report. Professor G. F. Lee, Civil and Environmental Engineering Department at the University of Wisconsin, provided the Hydro Products meter for the velocity measurements

TABLE OF CONTENTS

LIST OF FIGURES AND TABLES

INTRODUCTION

Waste water discharge into our oceans, estuaries, lakes, rivers and streams is a national problem, affecting not only public health but also the ecology and other potential uses of these water bodies. In the assessment of the effect of a waste water discharge on other uses of the receiving water body, an important consideration is the ability of the receiving water body to accept a certain amount of waste and through mixing and degradation processes reduce its concentration to an acceptable level. The mixing (dilution) process depends upon the physical and flow characteristics of the outfall, effluent and receiving water body.

During the summer of 1969, a field study of the effluent discharge from the Kraft Division of Consolidated Paper Company into the Wisconsin River at Wisconsin Rapids, Wisconsin, was undertaken (see Fig. 1). The Kraft Division is a new (built in 1967), bleached pulp mill having an average daily production of 315 tons of pulp and furnishing its treated process water and steam and electricity to the Wisconsin Rapids Division (the other mill of Consolidated Paper Company in Wisconsin Rapids). The Kraft Division mill also reuses some papermill whitewater from the Wisconsin Rapids Division for pulp washing. The kraft recovery process is used by the mill to reclaim chemicals and liquor from the pulp operations. Fibers are recovered from the wash waters by filters. Effluent and spills from process and

intake water clarification areas are collected and discharged over a riffler into a settling lagoon, having a detention time of approximately 12 hours. The lagoon discharges into the Wisconsin River through a 36-inch diameter concrete pipe (see Fig. 2). The lagoon is periodically cleaned by dredging and hauling to landfill. Cooking and storm waters are discharged directly to the Wisconsin River through a separate outfall (see Fig. 2).

This report presents the results of a field investigation carried out on September 12, 1969, to study the mixing (dilution) characteristics of this plant discharge. Boat measurements of the temperature and velocity distributions in the vicinity of the outfall were made. River, outfall and meteorological conditions were also monitored during the survey. In the analysis and interpretation of the field observations, several gross features of the effluent spreading and dilution processes have been examined (namely, the width, thickness, trajectory and centerline temperature variations of the effluent discharge with distance from the outfall). Comparison of these results with several "idealized" mathematical models and with laboratory experiments of others is also presented. Detailed mathematical modelling, including the actual river geometry and flow field, has not been undertaken. This modelling will be the subject of a later report. Finally, based upon the field observations and the analysis of this data, some comments are made on the mixing mechanisms

and on the size and shape of the mixing zone for the plant, river and weather conditions during the field survey.

The field work was carried out with the cooperation and support of the Consolidated Paper Company and the operating personnel at the Kraft Division Mill. This study, which was sponsored by DNR of the State of Wisconsin and NASA of the Federal Government, is part of the research project entitled "Definition of the Mixing Zone for Waste Effluents Discharged into Surface Waters".

The "mixing zone", as used herein, is the region of a water body in which a waste effluent, introduced into that environment, is diluted to the concentration level obtainable by complete mixing over a flow cross section of the water body at the point of discharge (for a river the flow cross section would be the river cross section at the outfall). The shape and extent of a mixing zone are dependent upon the type and the physical and flow characteristics of the effluent, outfall and receiving water body. The region downstream of a waste water discharge is usually divided into a near field region and a far field region. In the near field region which begins at the outfall, the momentum, discharge rate and buoyancy of the effluent, the shape and location of the outfall, and the interaction of these characteristics with the geometry of and the currents in the water body govern the rates of mixing (dilution) and spreading of the effluent in the water body. In the far field region which begins at the end of the near

field region, the continued mixing and spreading of the effluent in the water body is dominated by the currents, turbulence and geometry of the water body, by the outfall location and by the extent of and dilution in the near field region. The mixing zone, as defined above, generally encompasses the near field region and a portion of the far field region (note that dilution by mixing is a continuing process along a river channel). It is possible under certain circumstances that the near field region extends beyond the mixing zone.

Other definitions of a mixing zone such as the region in which a waste is diluted to a particular concentration could be used. The present State water quality guidelines only specify that a reasonable length, surface width or cross sectional area of a stream, river or lake may be used as a "mixing zone". The new Federal water quality guidelines will probably propose a mixing zone definition which is based upon the time of exposure of desirable organisms to detrimental concentrations.

The basic goals of this continuing investigation are to develop relationships for the extent and shape of the mixing zone in terms of outfall, effluent and water body characteristics and to apply remote sensing techniques to the determination of effluent concentrations in the mixing zone. Such relationships and techniques may be used: (1) in the establishment of definite and rational water quality guidelines; (2) in the development of sampling and regulation programs by government agencies; and (3) in the design and location of outfalls by industries and municipalities.

FIELD SURVEY

A. Site Location and Description

The location and general layout of the Kraft Division Consolidated Paper Company are shown in Figures 1 and 2. Pulp waste is discharged into the river through a 3-foot diameter concrete pipe, the top of which is submerged approximately 1.0 feet below river level. The outfall pipe is oriented perpendicular to the river bank as shown in Figure 2. Figure 3 is photographs of the river and outfall area, taken near the outfall discharge and looking toward the railroad bridge (the surface ripple and wave pattern in the foreground result from the submerged discharge; the culvert pipe at the bottom of the picture is an overflow pipe for the lagoon). The river is about 1250 feet wide at the outfall and the water level is maintained by a dam located approximately 3500 feet downstream (see Fig. 1). The river bottom slopes mildly downward (about 1:30) from shore where the water depth varies from 3-5 feet. The average river depth is 10 feet.

Approximately 1000 feet downstream from the outfall a railroad bridge crosses the river. Part of this bridge is composed of an earth fill which blocks about 1/3 the width of the river near the north shore (see Figs. 2 and 3). There is a small flow passage between the north shore and the earth fill, but the majority of the river flow is channeled through the larger opening on the south side of the river.

B. Characteristics of Plant Operation, River and Weather During Survey

A summary of river and effluent characteristics is given in Table I. The hourly river flow rate measured by the U.S.G.S. gaging station at Wisconsin Rapids (Fig. 1) is shown in Table II.

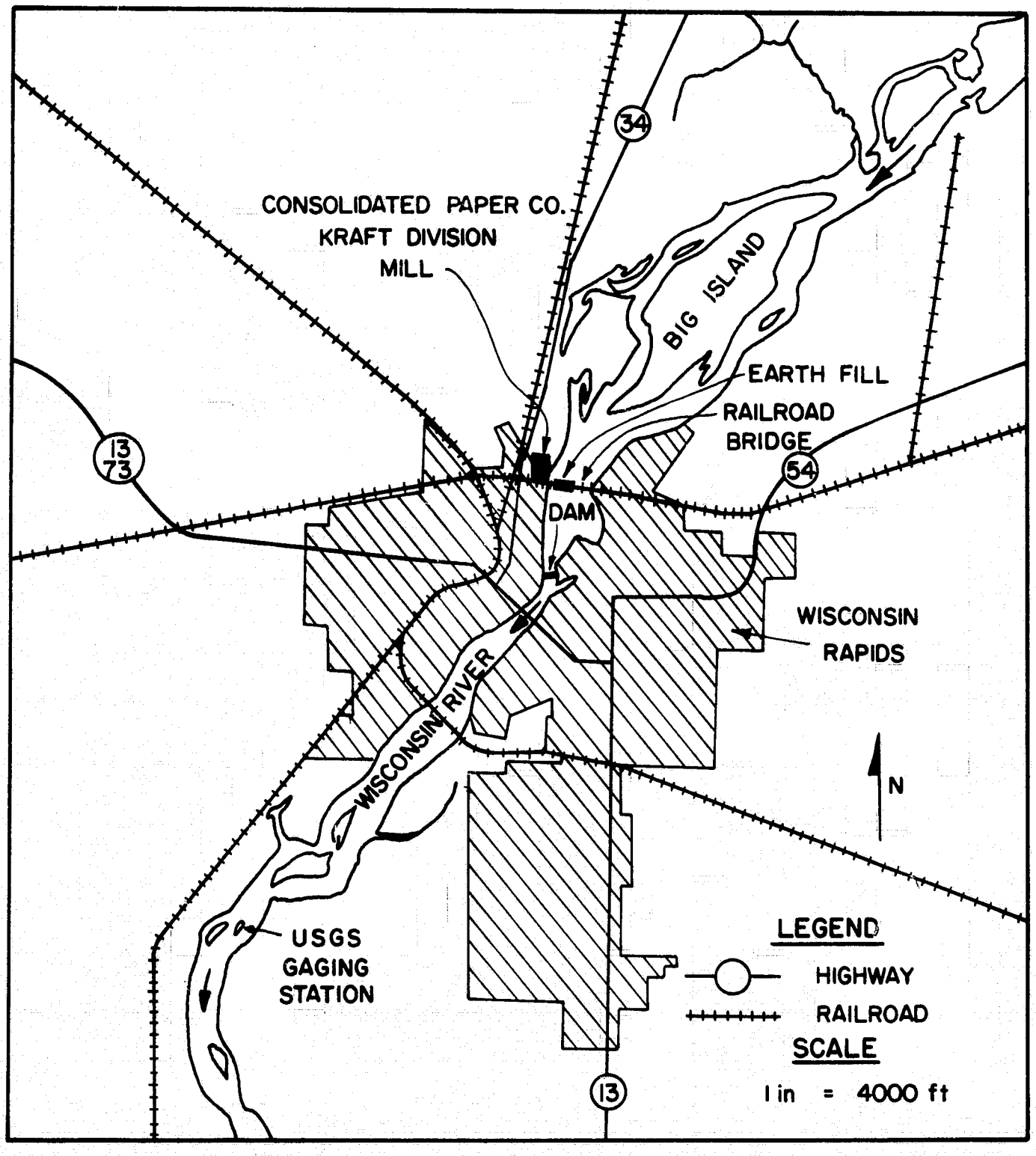

Fig. 1 Location Map

Fig. 2 General Layout of the Site

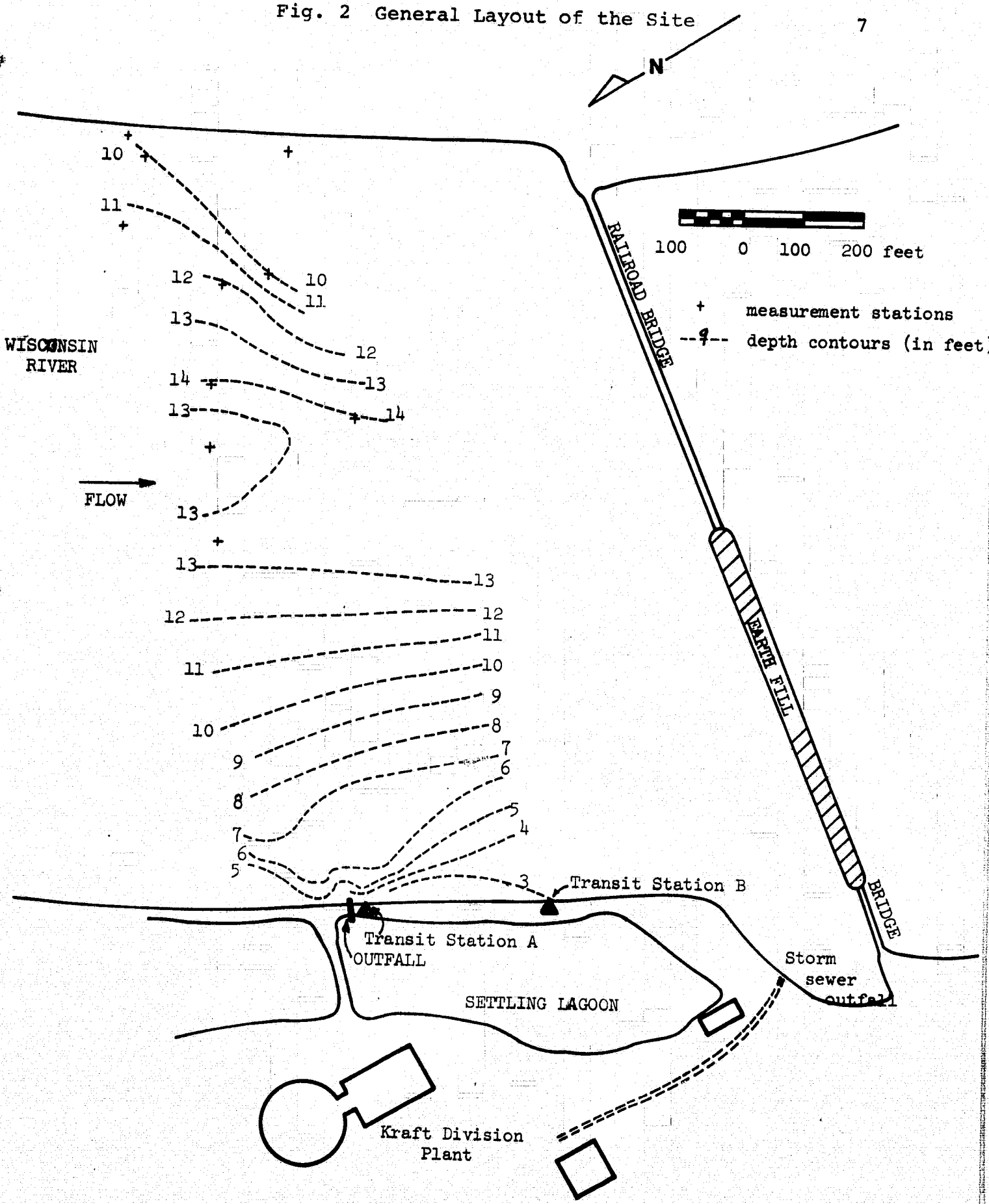

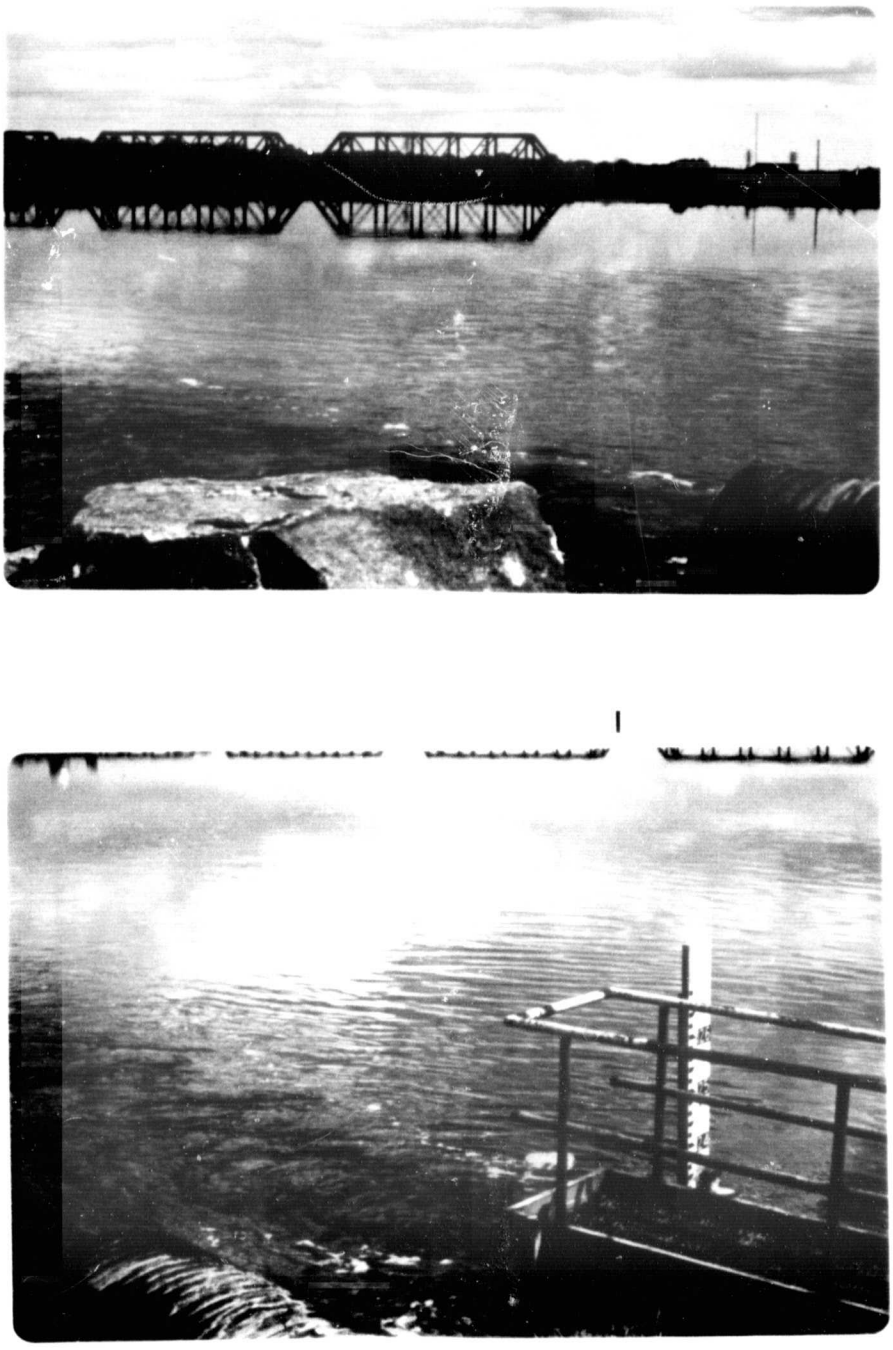

Fig. 3 Color Photographs of River and Outfall Area

TABLE I SUMMARY OF RIVER, WEATHER AND PLANT CONDITIONS FOR SEPTEMBER 12, 1969, SURVEY

RIVER AND WEATHER DATA
River width - 1,250 ft.
River depth - 10 ft.
Flow rate - 2,700 cfs
Characteristic velocity, V_r, - 0.22 fps
Reynolds number - 220,000
Froude number - 0.012
Water Temperature - 21.2°C - 19.4°C (top to bottom)
Wind - windy (blowing upstream), 10-15 mph
Density - 0.998
EFFLUENT AND OUTFALL DATA
Type of effluent - Pulp process water
Shape and size of outfall - circular, 3 ft. dia.
Discharge - 19.2 cfs
Discharge velocity, u_o, - 2.72 fps
Velocity ratio, u_o/V_r, - 12.4
Reynolds number of outfall - 800,000
Densimetric Froude number of outfall - 6.0
Effluent temperature - 40°C
Density - 0.996

TABLE II HOURLY WISCONSIN RIVER FLOW FOR SEPTEMBER 12, 1969 AT U.S.G.S. GAGING STATION IN WISCONSIN RAPIDS

Time	Flow, cfs	
9 A.M.	3058	
10	3058	
11	2863	
12	2863	
1 P.M.	2680	
2	2731	Survey Period
3	2697	
4	2697	
5	2697	
6	2697	
7	2697	
8	2697	
9	2697	
10	2694	

The U.S.G.S. Gaging Station at Wisconsin Rapids is located at latitude 44°22'05" and longitude 89°51'30" (see Fig. 1).

It can be seen that the total effluent discharge (19.2 cfs) is less than 1% of the river flow (2700 cfs); however, the velocity of the effluent is approximately 13 times that of the river. The river was slightly temperature stratified (21.2°C top, 19.4°C bottom) and the effluent (40°C) was approximately 0.3% lighter than the river and hence buoyant. Effluent temperature and discharge were monitored periodically throughout the survey period (2 pm-7 pm).

C. Experimental Procedures and Equipment

Data acquisition was accomplished using a 12-foot, row boat and motor and consisted of measurements of velocities and temperatures at 45 different river positions (Fig. 2 shows some of the locations). At each measurement position the boat was anchored, and upon a flag signal, transit sightings on the bow of the boat were simultaneously taken from two shore stations (A and B, see Fig. 2). The transit sightings consisted of angle measurements from the baseline between the two instrument stations to the boat and the time and number of each sighting (for correlation and plotting purposes later). At each position, the vertical distributions of velocity and temperature over the river depth were measured.

A Hydro Products pulse rate current meter (suspended on a calibrated cable) was used to make velocity measurements at 1 to 2 foot depth increments below the water surface. This meter was accurate to within $\pm$0.2 feet per second. To determine current directions the current meter vane was aligned with the north arrow on a compass dial and the current direction with respect to magnetic north was read to the nearest 10 degrees.

A Whitney underwater thermometer (model TC5, No. 66S8) was used for temperature measurements. The accuracy of this thermometer was 0.1°C. Temperatures were measured at 1/2 to 1 foot depth increments below the water surface.

The transit crew periodically monitored the effluent temperature and specific gravity at the outfall using a Whitney underwater thermometer and a Westphal Balance (Fisher Scientific Co., No. 683).

D. Data Reduction

The primary objective in the data reduction was to obtain the concentration patterns resulting from the mixing of the effluent within the river. From the concentration patterns, variations of the trajectory, width, thickness and maximum temperature of the effluent discharge with distance from the outfall were obtained. In this work, the temperature rise above the river is used as a tracer of the discharge. Thus the relative effluent concentration at any point was determined from the temperature measurements using the relation

$$\frac{c}{c_o} = \frac{T-T_r}{T_o-T_r}, \qquad (1)$$

where c is the concentration at any point, c_o is the effluent concentration at the outfall, T is the temperature at any point, T_r is the undisturbed river temperature, and T_o is the effluent temperature at the outfall. Concentration (temperature) contours were developed from plots of the measured temperature concentrations using a linear interpolation between adjacent measurements. Patterns of concentration (temperature) contours on horizontal planes below the water surface, on the vertical plane through the effluent discharge centerline and on vertical planes perpendicular to the effluent discharge centerline are given in the next section.

Distributions of velocity on the water surface and over the depth were developed from plots of the measured velocities. These velocity patterns are presented in the next section.

The location of each position at which the vertical distribution of temperature and velocity were measured was determined by angular intersection of the transit observations. The angular measurements to the boat from each transit station were plotted on a scale map; the intersection of the lines of sight from the two transit stations determined the boat (and measurement station) location.

Several vertical temperature distributions measured outside the effluent discharge region are shown in Figure 4. It was found that a slight temperature stratification existed in the undisturbed river water and that surface temperatures were nearly uniform at about 20.7°C while bottom temperatures were nearly uniform at about 19.5°C. It was then assumed that these conditions would be typical of the river in the absence of the effluent discharge. Further, the river temperature distributions inside the effluent discharge region were approximated by a simple parabola

$$T_r = 20.7 - 1.2\left(\frac{z}{d}\right)^2 , \qquad (2)$$

where z is the depth at which the temperature is measured and d is the river depth at that point. It was found that the temperature given by Eq. 2 was always within 0.6°C of the actual temperature distributions measured in the undisturbed river.

During the survey the outfall temperature, T_o, fluctuated over several degrees as shown in Figure 5. For data reduction, the average value of 40.3°C was used. The specific gravity of the effluent also varied over the survey period as shown in Figure 6. For data reduction, the average value of 0.996 has been used.

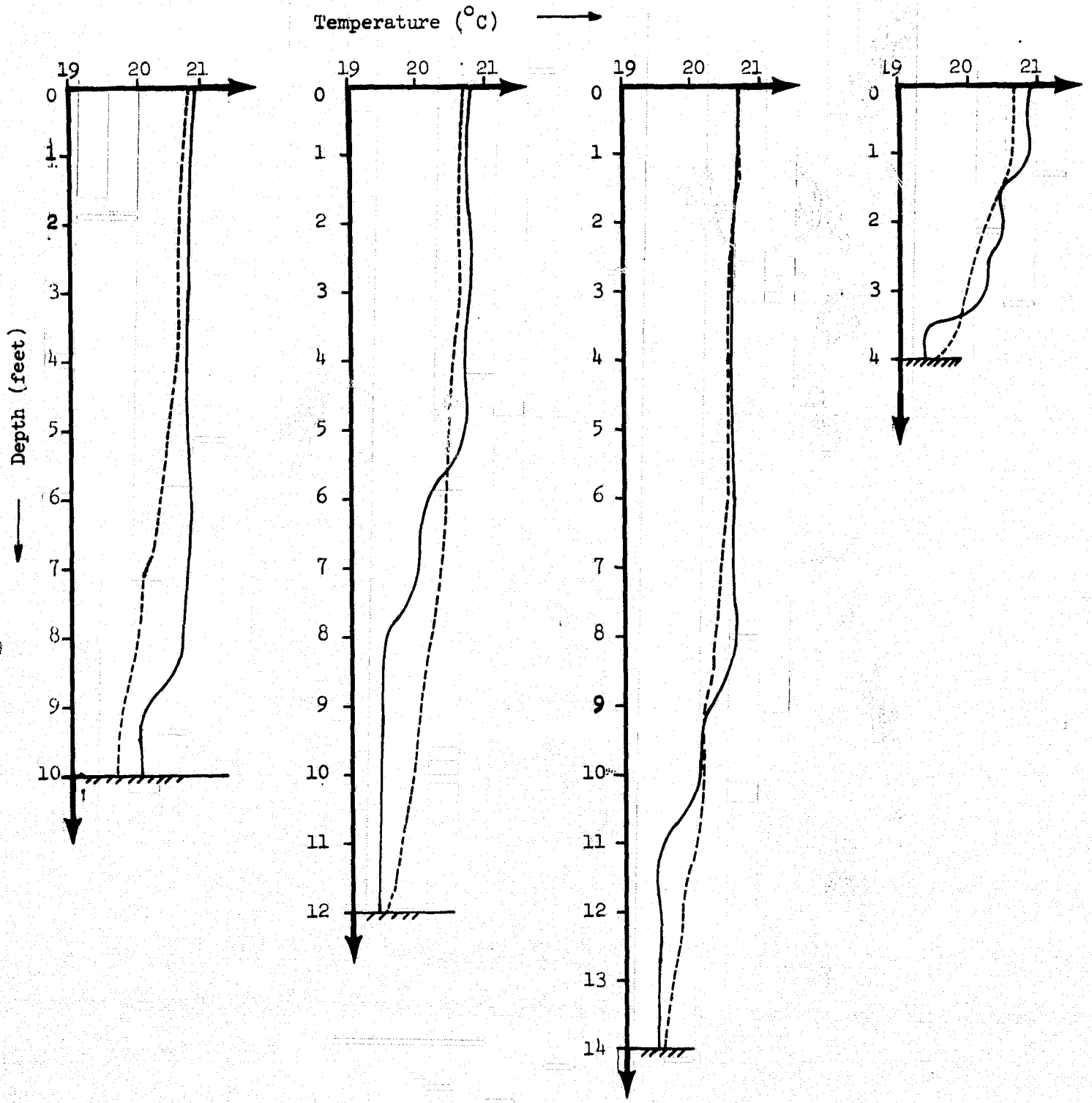

Solid line : Measured Temperature Distribution
Dash line : Assumed Temperature Distribution

Fig. 4 Temperature Distribution at Selected Points Outside the Effluent Discharge Region

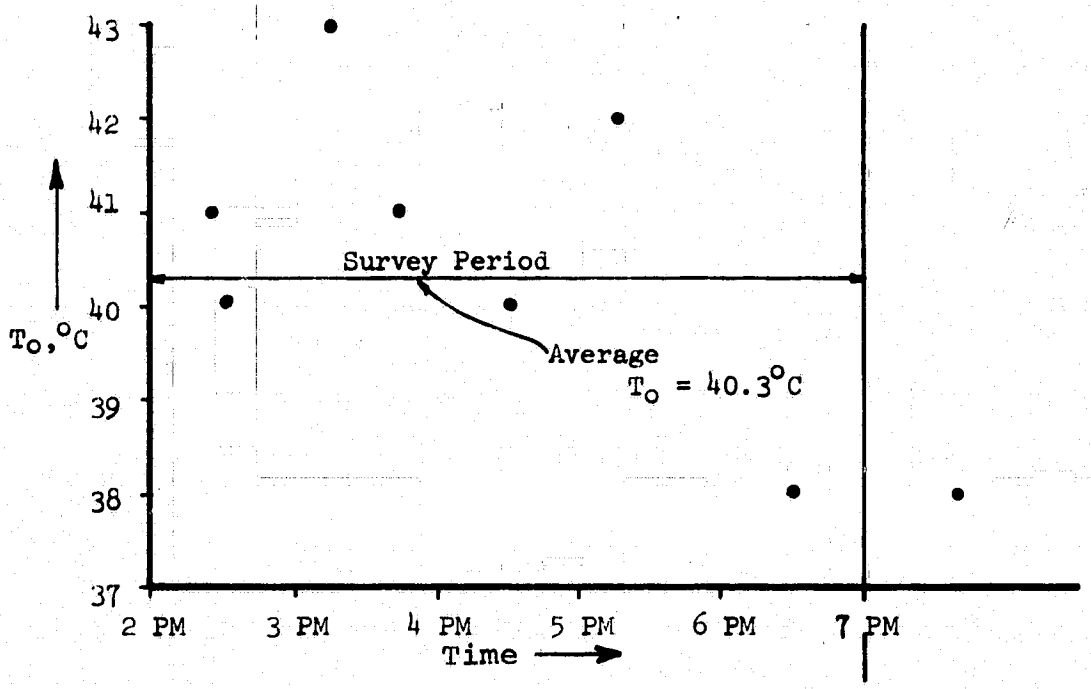

Fig. 5 Effluent Temperature during Survey Period

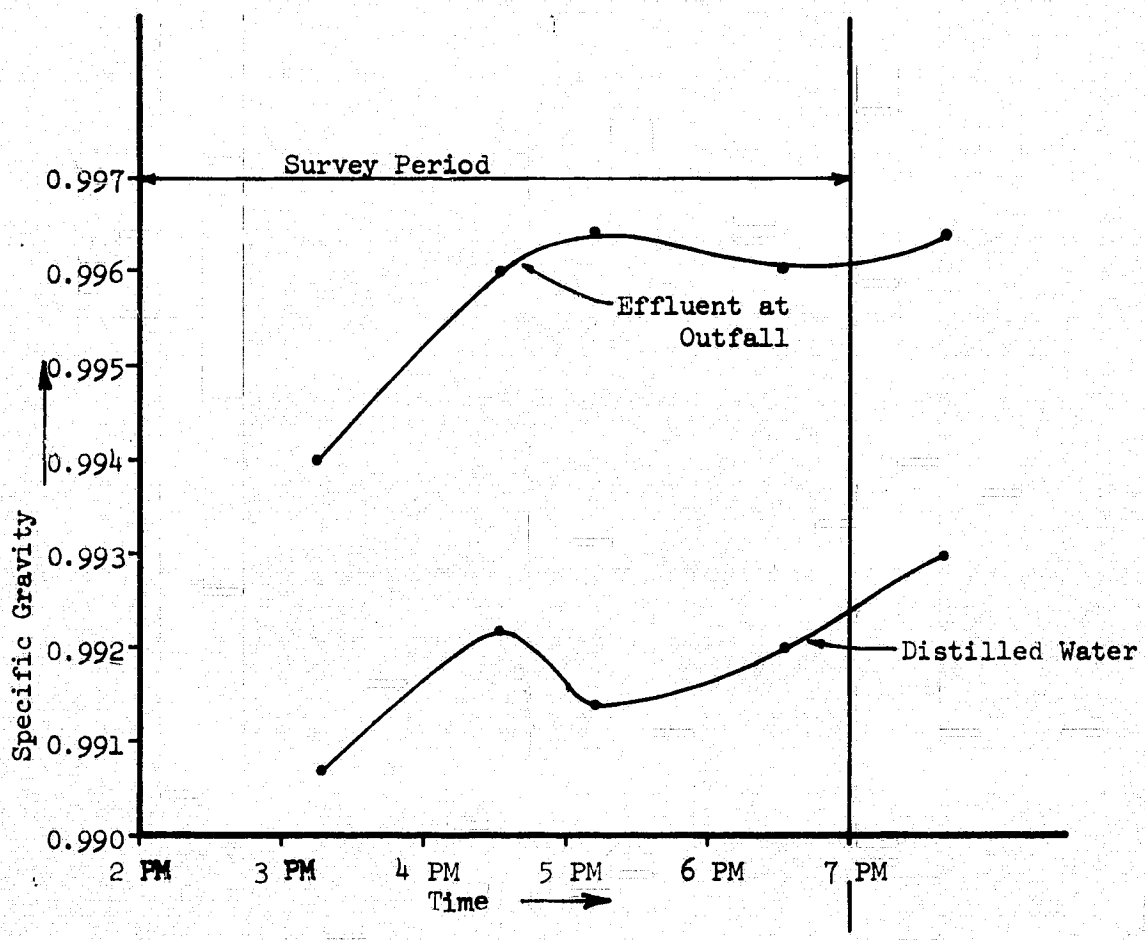

Fig. 6 Specific Gravity of Effluent and Distilled Water at Same Temperature

PRESENTATION AND DISCUSSION OF FIELD OBSERVATIONS

Average river flow and effluent discharge conditions over the survey period are summarized in Table I. The effluent discharge (supplied by the Kraft Division of Consolidated Paper Company) was an average value over 24 hours of operation (no periodic measurements were made). The specific gravity of the effluent as determined from periodic sampling is shown in Fig. 6. Also shown for comparison is the specific gravity of distilled water at the same temperature. The effluent was 0.3 - 0.5% heavier than distilled water due to suspended material in the effluent. However, due to its temperature, the effluent was about 0.2% lighter than the ambient river water.

A. Distribution of Temperature on Horizontal Planes

Concentration contours on horizontal planes at several depths below the water surface are shown in Figs. 7-11. These figures show that the effluent discharge spreads laterally very rapidly close to the outfall. This spreading is faster than for a simple jet discharge (1,2,4) and is due, as discussed further in the next section, to the shallow depths, to the river flow and to the density difference between the effluent and the river. It can also be seen in these figures that buoyancy is an important force close to the outfall (less than about 30 feet from the outfall) as the effluent moves rapidly upward to form a surface layer. This effect of buoyancy can be readily seen in Fig. 12 which shows the concentration distribution on a vertical section through the centerline of the effluent discharge (the centerline of the effluent discharge, shown on Fig. 7, was defined as the line through the maximum concentration in a

Fig. 7 Concentration Pattern (Surface)

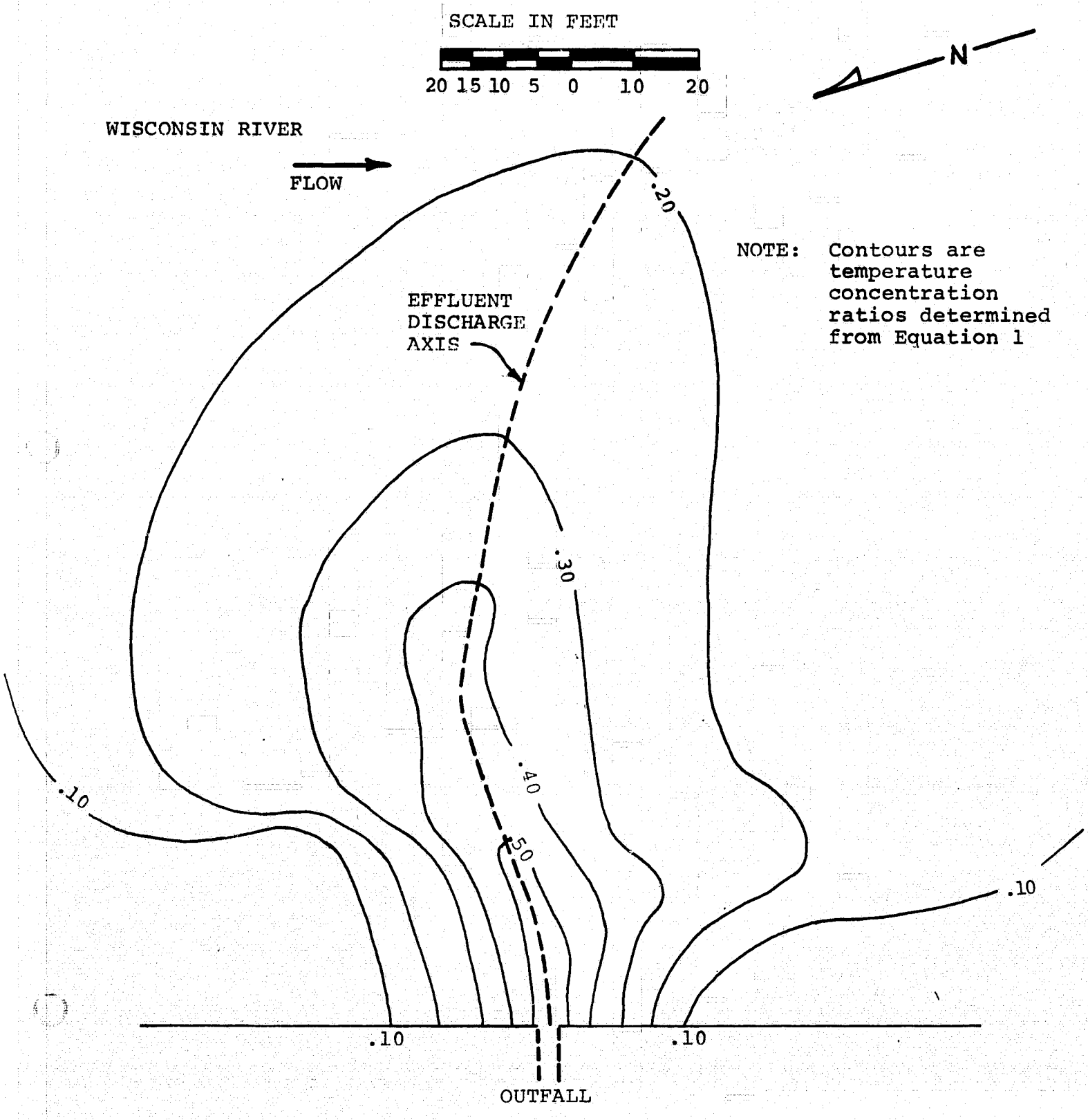

Fig. 8 Concentration Pattern (1 Foot Below Surface)

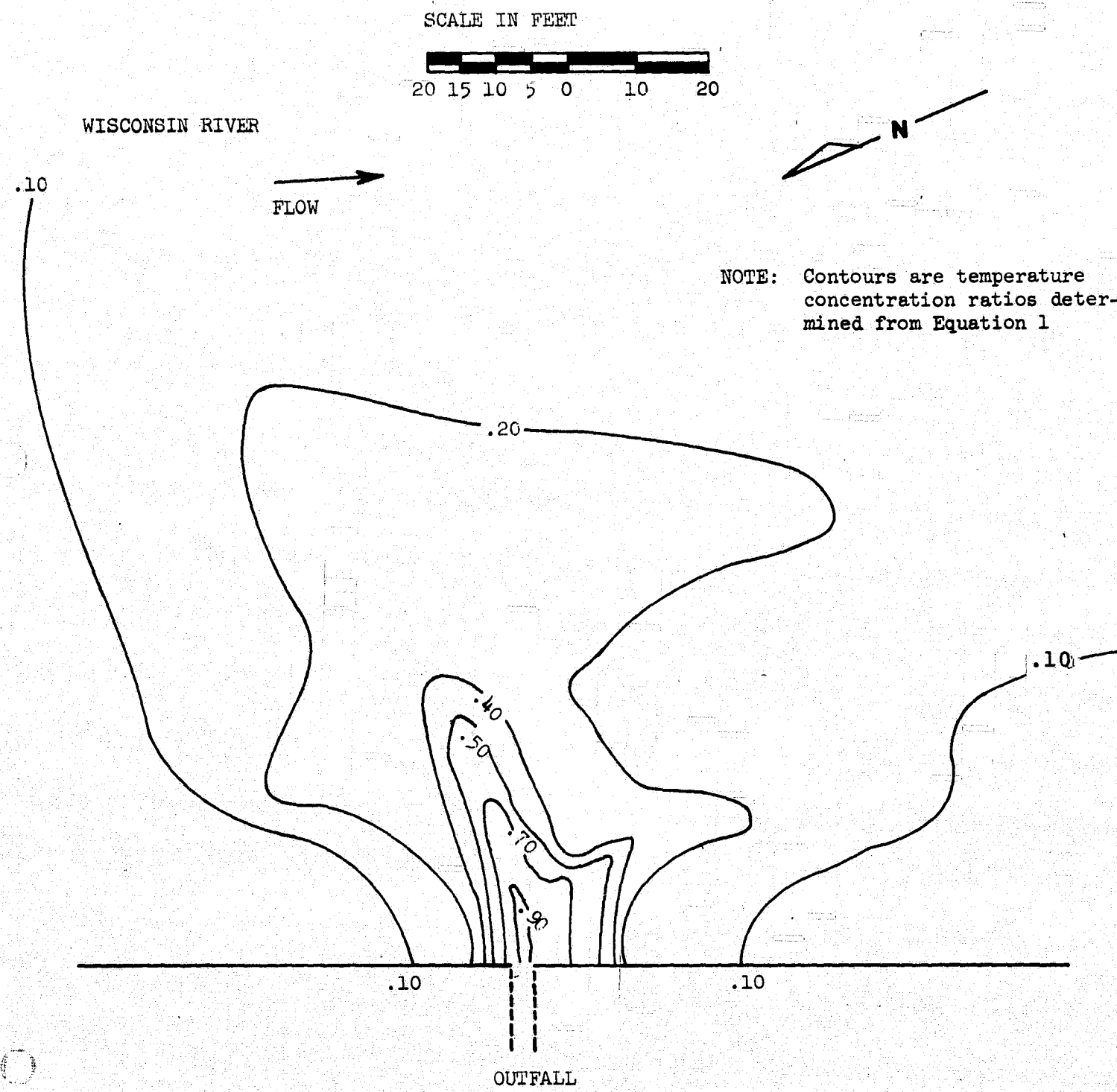

Fig. 9 Concentration Pattern (2 Foot Below Surface)

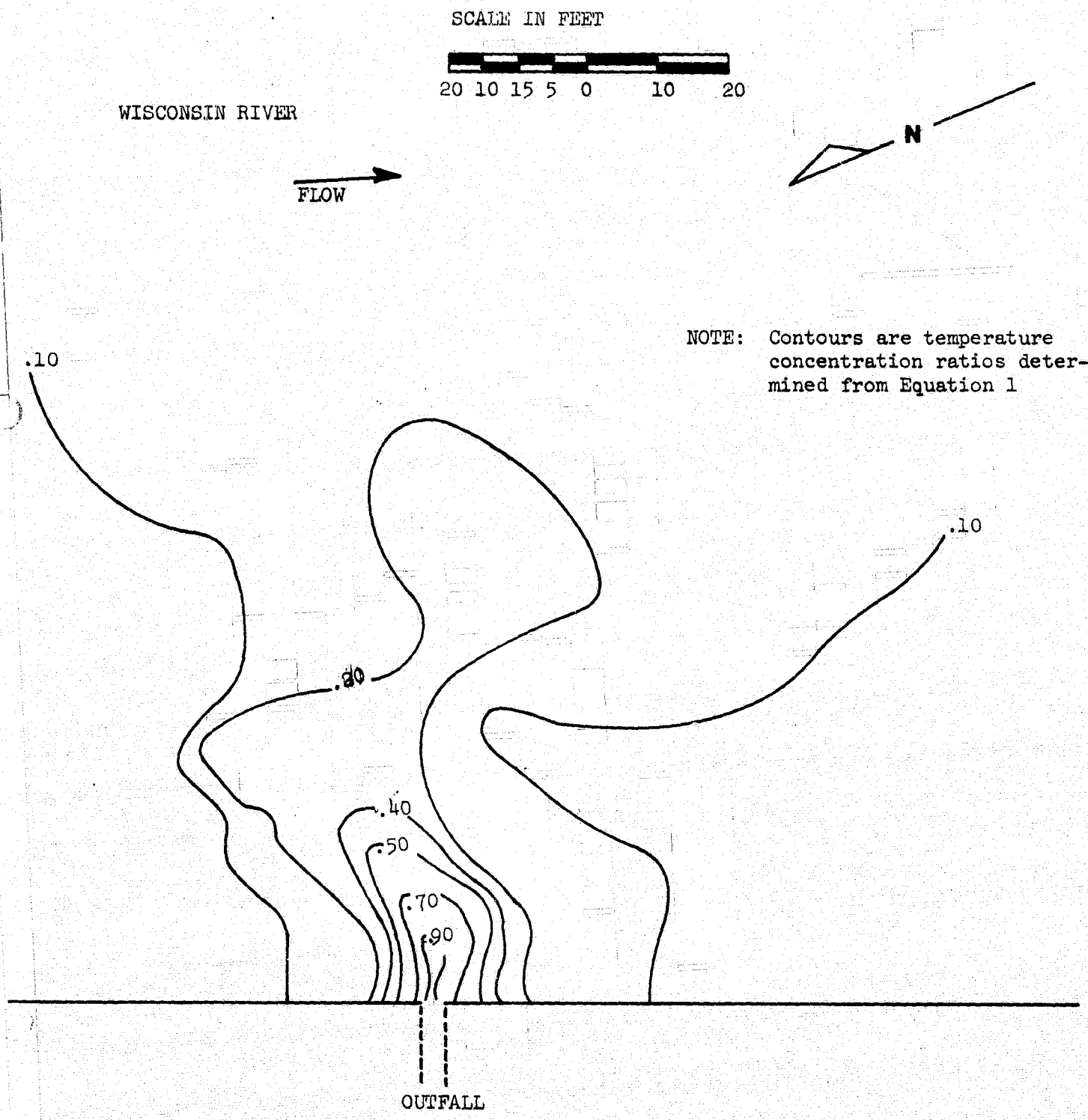

Fig. 10 Concentration Pattern (3 Foot Below Surface)

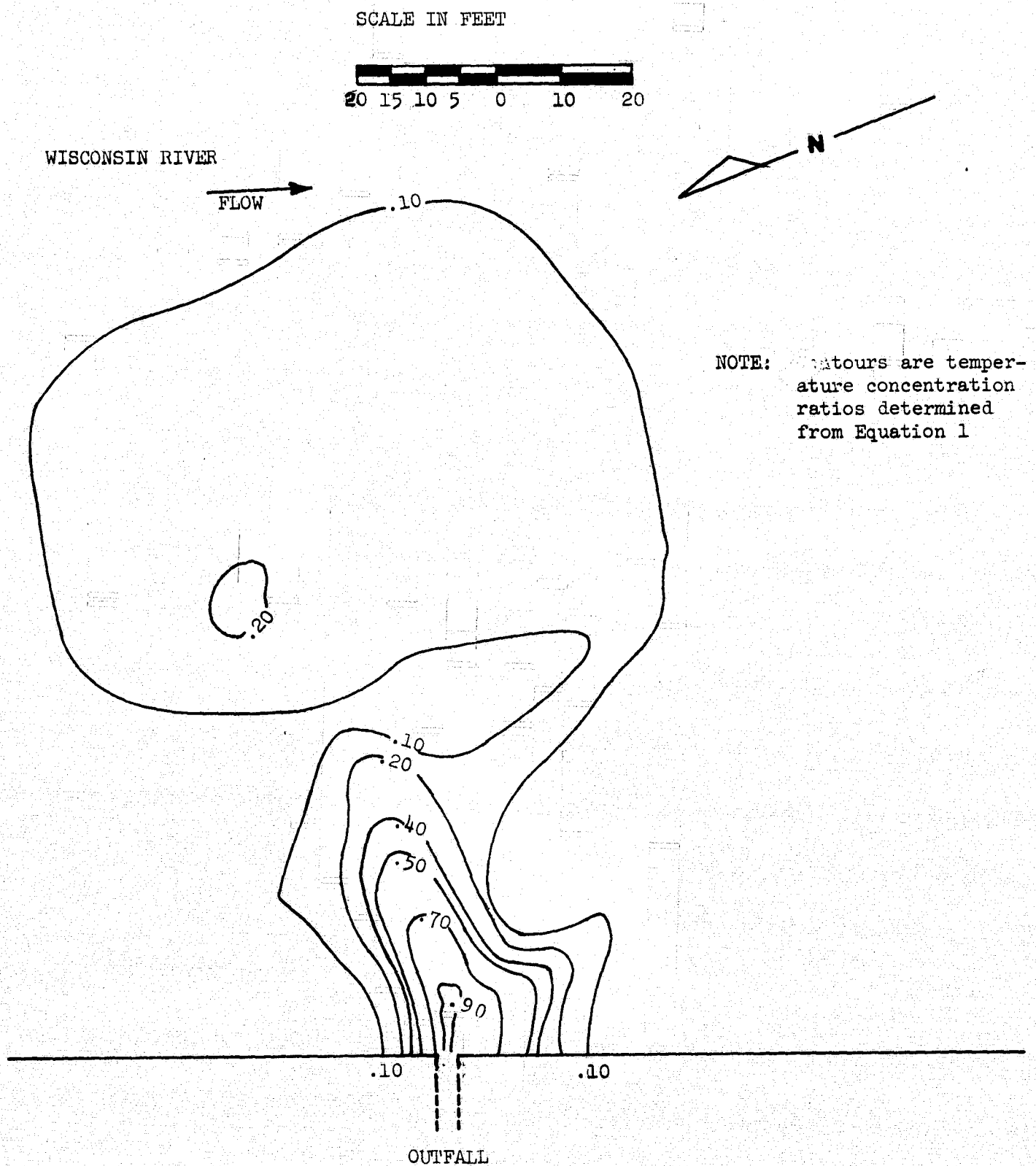

NOTE: Contours are temperature concentration ratios determined from Equation 1

Fig. 11 Concentration Pattern (4 Foot Below Surface)

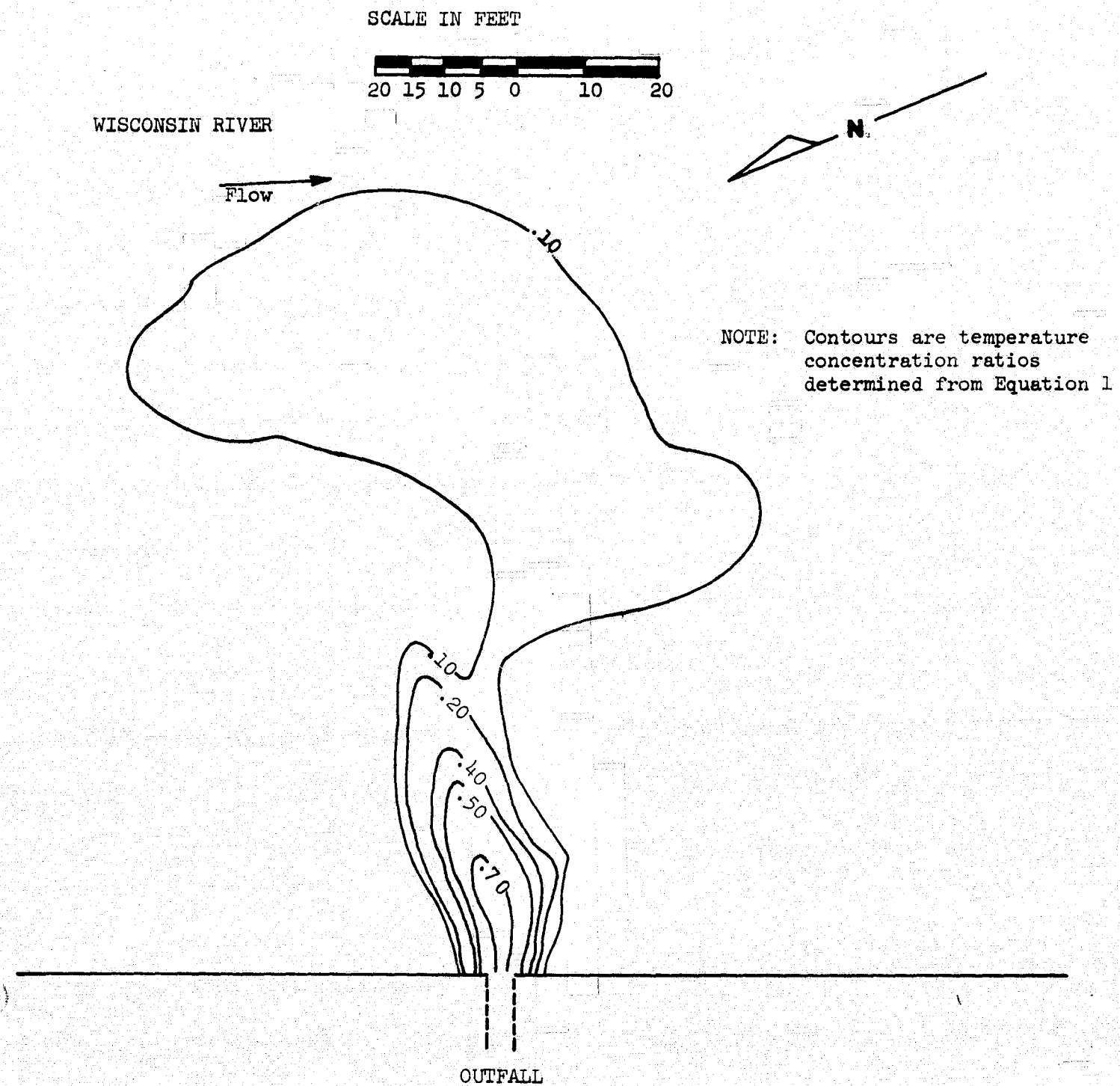

NOTE: Contours are temperature concentration ratios determined from Equation 1

vertical cross section of the effluent discharge). Beyond this initial region the effluent discharge centerline remains on the water surface.

B. Distribution of Temperature along Vertical Plane through Discharge Centerline

In the submerged region, there were not sufficient measurements to determine the locus of the effluent discharge centerline (i.e., first 24 feet from the outfall), and the location of the concentration contour lines had to be estimated. The effluent discharge centerline in this region (see Fig. 12) was determined by an approximate analysis of the dynamics of a fluid particle. The assumptions and equations used in this analysis are described below.

Since the mean velocity in the river is low (0.22 fps), the buoyant force and the initial discharge momentum predominate in the determination of the effluent discharge centerline in the submerged region (i.e., the effect of river flow on the locus of the centerline can be neglected). A fluid particle moving along the centerline is assumed to have the same horizontal velocity as a fluid particle moving along the centerline of a simple momentum jet (i.e., no buoyancy or boundary effects). Albertson et al. (2) give the following expressions for the horizontal velocity of a simple jet: in the zone of flow establishment

$$u_m = u_o \tag{3}$$

and in the zone of established flow

$$u_m = \frac{6.2D}{x} u_o, \tag{4}$$

where u_m is the horizontal velocity component along the jet centerline, u_o is the velocity at the outfall, D is the diameter

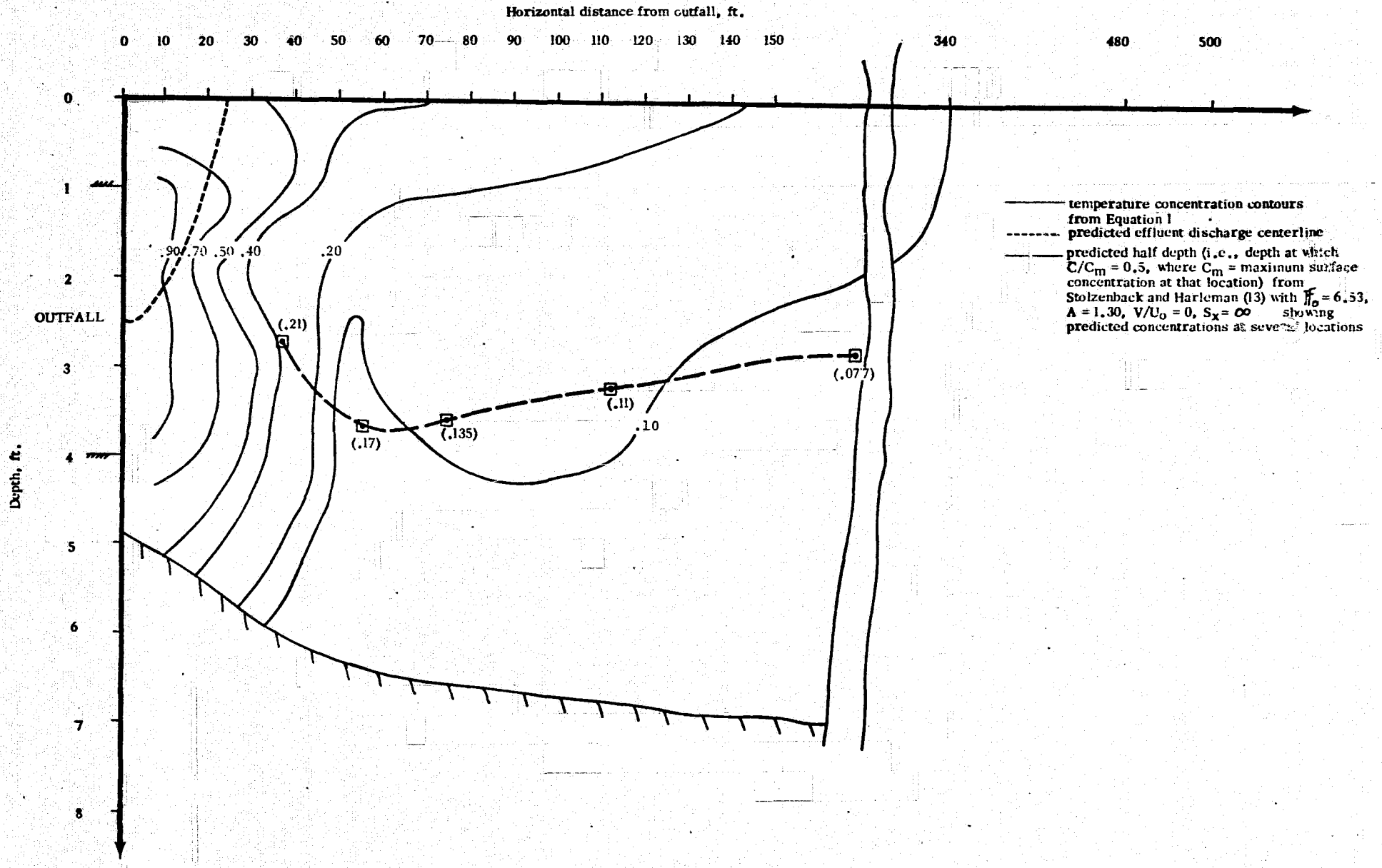

Fig. 12 Temperature Concentration Contours on Vertical Section through Effluent Discharge Axis

of the outfall, and x the horizontal coordinate as shown in Fig. 13. The length of the zone of flow establishment is assumed to be $x = 6.2D$ (see (2)).

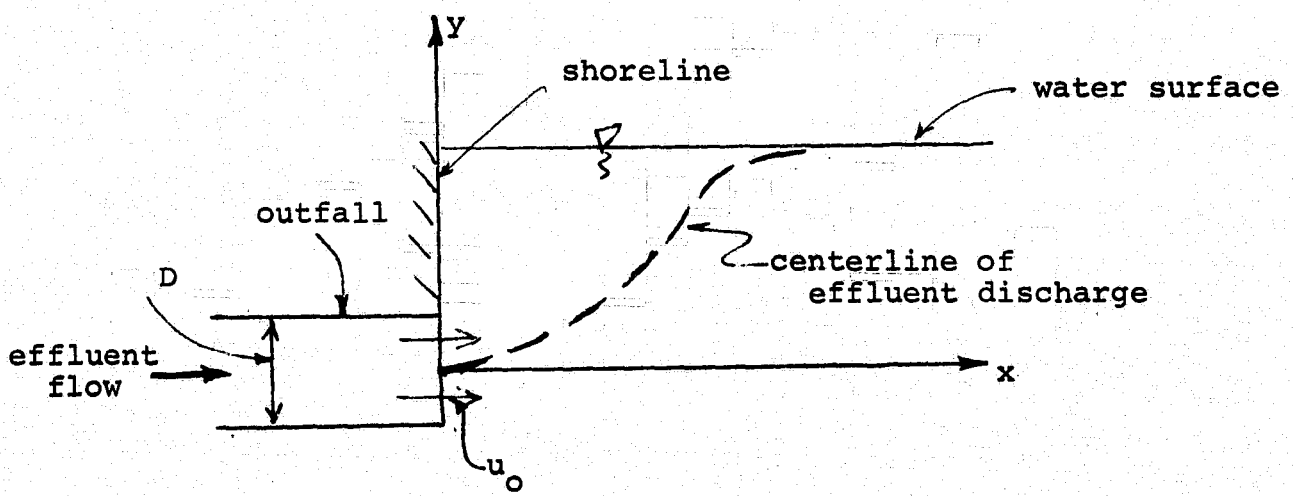

Fig. 13 - Definition Sketch for Effluent Discharge Centerline in Submerged Region

In addition to its horizontal momentum, the effluent discharge is also deflected upward by the buoyant force. Assuming that the density difference between the effluent and the river of a fluid particle decreases in the same manner as the velocity along the axis of a simple jet, we have for the zone of flow establishment

$$\frac{\rho_m - \rho_r}{\rho_r} = \frac{\rho_o - \rho_r}{\rho_r} \qquad (5)$$

and for the zone of established flow

$$\frac{\rho_m-\rho_r}{\rho_r} = \frac{\rho_o-\rho_r}{\rho_r}\left(\frac{6.2D}{x}\right), \tag{6}$$

where ρ_m is the density of a particle along the effluent discharge centerline, ρ_o is the density of the effluent, and ρ_r is the density of the river water. Now, due to buoyancy, the vertical force/unit mass on a fluid particle moving along the centerline is given by

$$F_y = \frac{\rho_m-\rho_r}{\rho_r} g. \tag{7}$$

Hence, the trajectory of a fluid particle is defined by

$$\frac{dx}{dt} = u_m \tag{8}$$

$$\frac{d^2y}{dt^2} = a_y = \frac{\rho_m-\rho_r}{\rho_r} g, \tag{9}$$

subject to the following boundary conditions

$$\text{at } t = 0,\ x = 0,\ \frac{dy}{dt} = 0,\ y = 0 \tag{10}$$

The locus of the centerline in the zone of flow establishment can be determined by substituting eq. (3) into eq. (8), eq. (5) into eq. (9) and applying the boundary conditions in (10). The result is

$$y = 1/2\left(\frac{\rho_o-\rho_r}{\rho_r} g\right)x^2/u_o^2 \quad . \tag{11}$$

At the end of zone of flow establishment,

$$x_e = 6.2D$$

$$y_e = 19.2\left(\frac{\rho_o-\rho_r}{\rho_r} g\right)D^2/u_o^2 \qquad (12)$$

$$v_e = \frac{(\rho_o-\rho_r)g}{\rho_r}\frac{6.2D}{u_o}$$

$$u_{m_e} = u_o,$$

where v_e = vertical velocity.

For the zone of established flow, substituting eq. (4) into eq. (8), and eq. (6) into eq. (9) and applying the boundary conditions shown in eq. (12) leads to the following result for the trajectory

$$y = \frac{1}{18.6}\left(\frac{\rho_o-\rho_r}{\rho_r}\right)\frac{g}{u_o^2 D}x^3 + 6.4\left(\frac{\rho_o-\rho_r}{\rho_r} g\right)\frac{D^2}{u_o^2}. \qquad (13)$$

The centerline shown in Fig. 12 was determined by eqs. (11) and (13) for the two different zones, respectively. This simple analysis predicts the surface intersection point to be 24 feet from the outfall which compares favorably with the field observations. More detailed and complete analyses for the characteristics and trajectories of buoyant jet discharges are given in (1) and (4).

C. Distribution of Temperature in Planes Perpendicular to Discharge Centerline

Several cross sections normal to the effluent discharge centerline at different distances from the outfall are shown in Figs. 14 - 17. These sections are drawn looking from the outfall into the river, hence the river downstream is to the right on these sections. The concentration contours are not symmetric

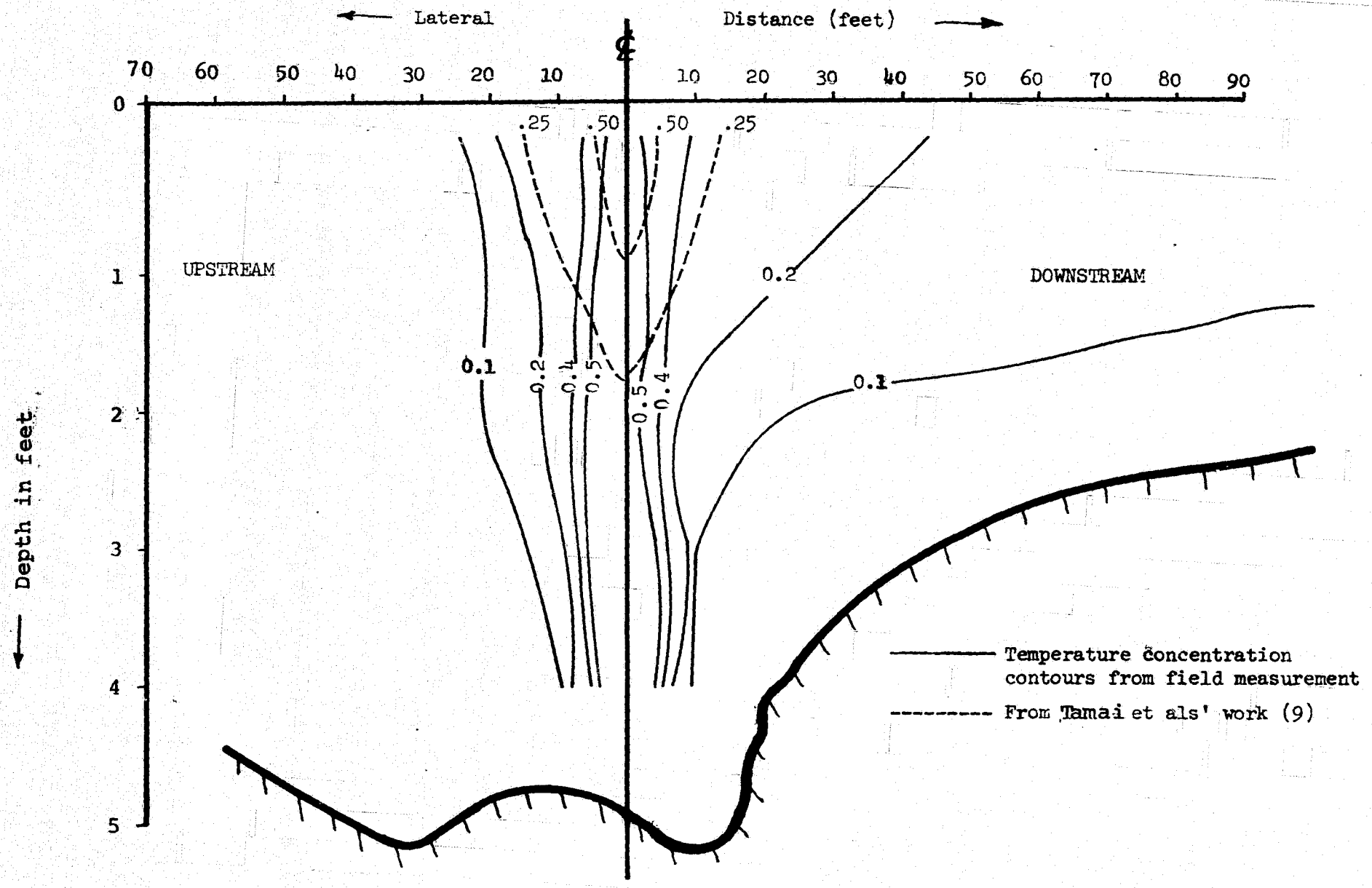

Fig. 14 Cross Sectional Distribution of Concentration 20 Feet from Outfall Perpendicular to Discharge Axis

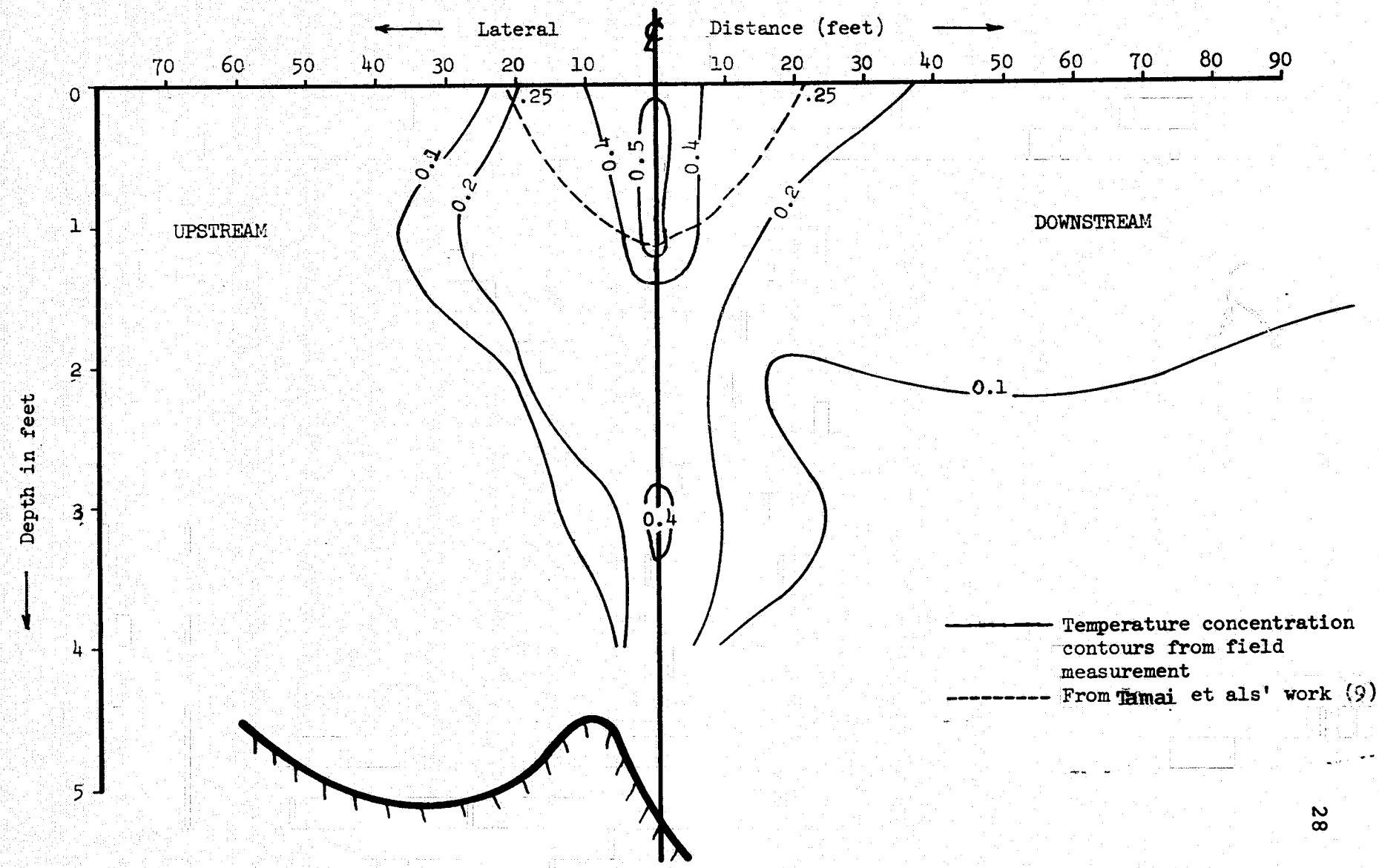

Fig. 15 Cross Sectional Distribution of Concentration 34 Feet from Outfall Perpendicular to Discharge Axis

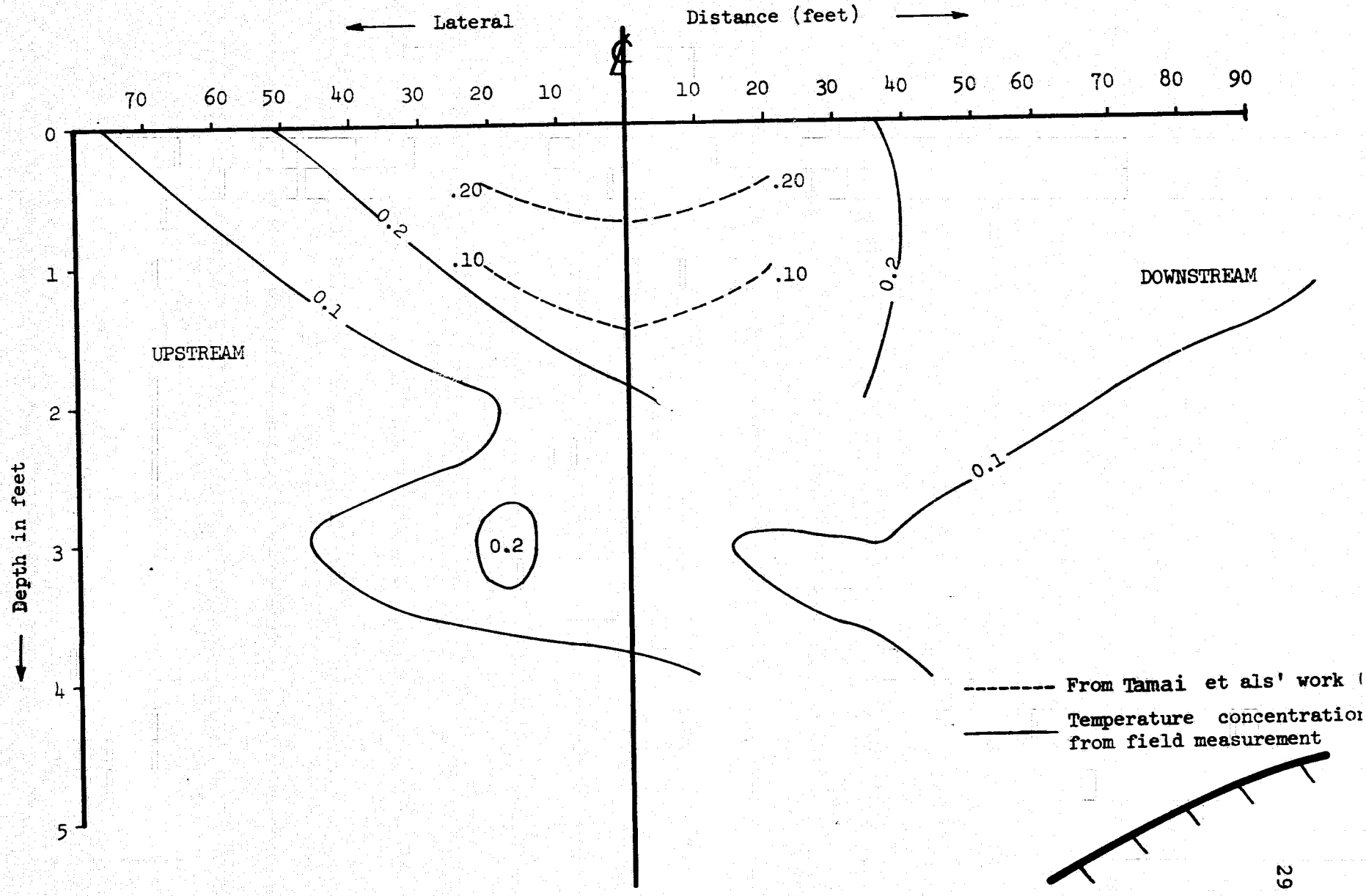

Fig. 16 Cross Sectional Distribution of Concentration 64 Feet from Outfall Perpendicular to Discharge Axis

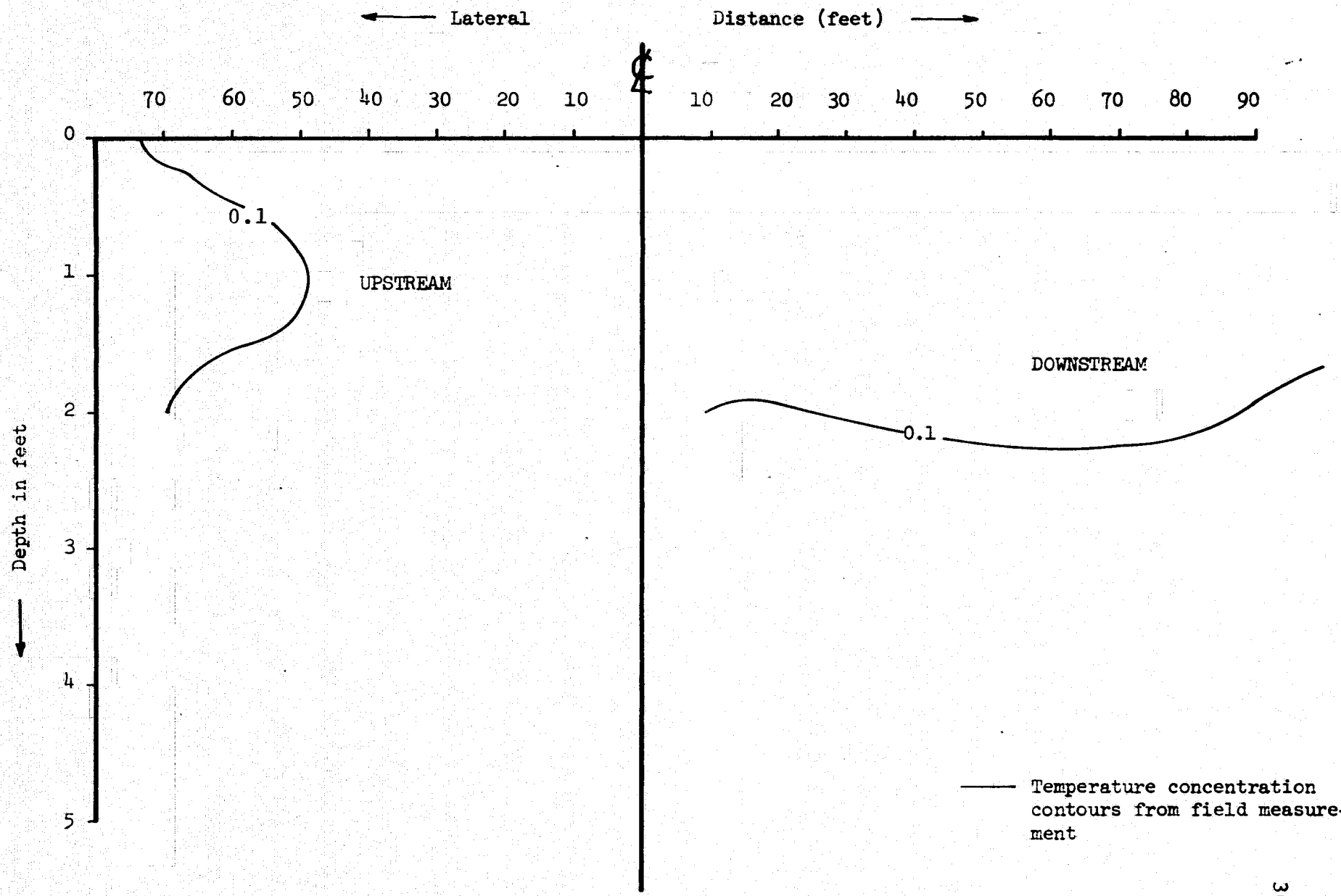

Fig. 17 Cross Sectional Distribution of Concentration 156 Feet from Outfall Perpendicular to Discharge Axis

with respect to the jet axis. Concentration gradients are steeper on the upstream side than on the downstream side of the effluent discharge.

D. Distribution of Velocity within Discharge

The velocity measurements were not sufficiently detailed to develop cross sectional distributions similar to those for temperature in Figures 14-17. However, vertical distributions of velocity at various locations are plotted in Figure 18 along with the temperature concentration distributions at the same locations. Theoretically, the velocity distribution and concentration distribution should be of the same shape at the same location. In Figure 18a the two distribution curves are very similar in shape. The velocity magnitudes show that this location, as expected, is in the zone of flow establishment, where velocities at depths from about 2 feet to 3 feet (i.e., in the potential core) should be equal to the discharge velocity of 2.72 fps. The differences between the expected and measured distributions could be due to errors in the measurements and to vertical motions resulting from the buoyancy of the discharge. At the other two locations shown in Figure 18b and c the shapes of the concentration and velocity curves are similar over most of the depth. The differences in the shapes of the distributions could be due to errors in measurement (particularly velocity) and the fact that the depth increments for the measurements of velocity and of concentration were not the same.

Figure 19 shows the surface pattern (actually 1/2 foot below the water surface) of measured velocities (both magnitude and

direction) in the vicinity of the outfall. The apparent discrepancy in direction between some of the adjacent measurements results from the fact that these measurements were made at different times throughout the survey period and the effluent and/or ambient conditions had changed between the two measurements. Apart from these discrepancies, however, the measurements show the rapid spreading of the effluent discharge close to the outfall, noted in the temperature distributions of Figures 7-11. Away from the outfall, the velocity measurements give an indication of the river currents, though the measurements are not sufficient to define the river flow pattern in detail.

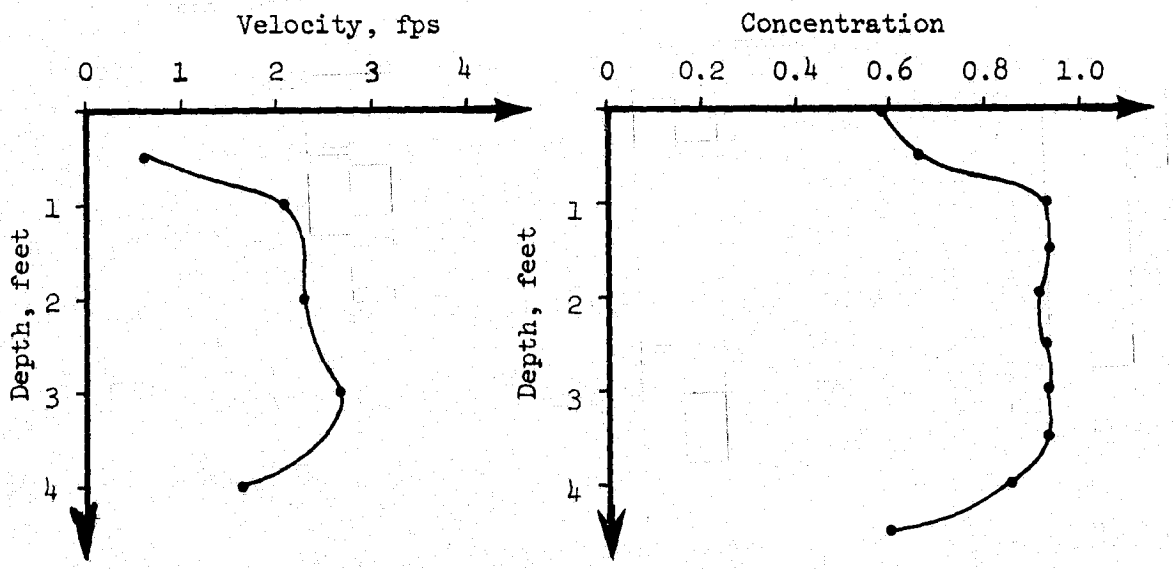

a) A point 10 ft from outfall along the effluent discharge centerline.

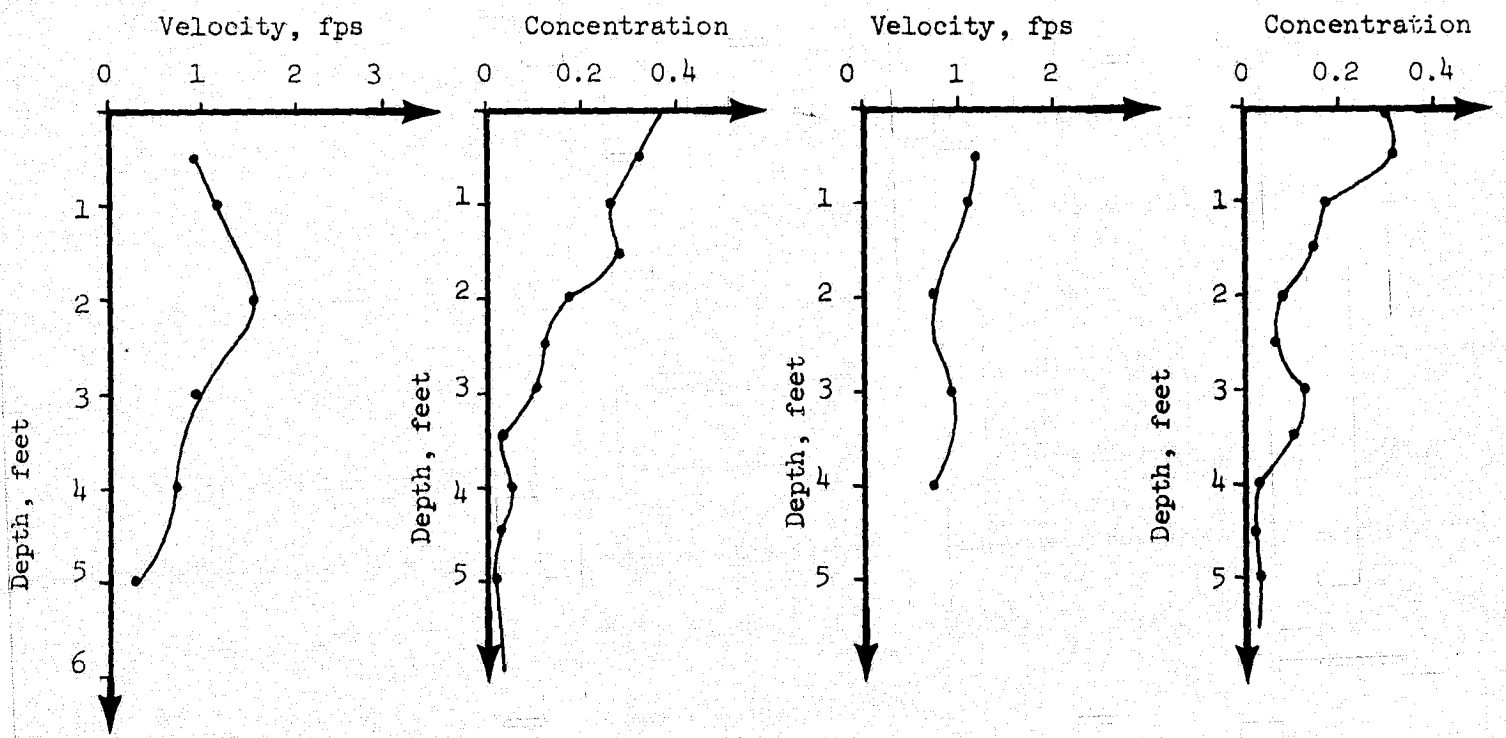

b) A point 10 ft downstream from the effluent discharge centerline and 42 ft from the outfall along the centerline.

c) A point 20 ft downstream from the effluent discharge centerline and 35 ft from the outfall along the centerline.

Fig. 18 Vertical Distributions of Velocity and Concentration at Several Locations in the Effluent Discharge

Scales

Geometry - 1 in = 100 ft
Velocity - 1 in = 2 ft/sec

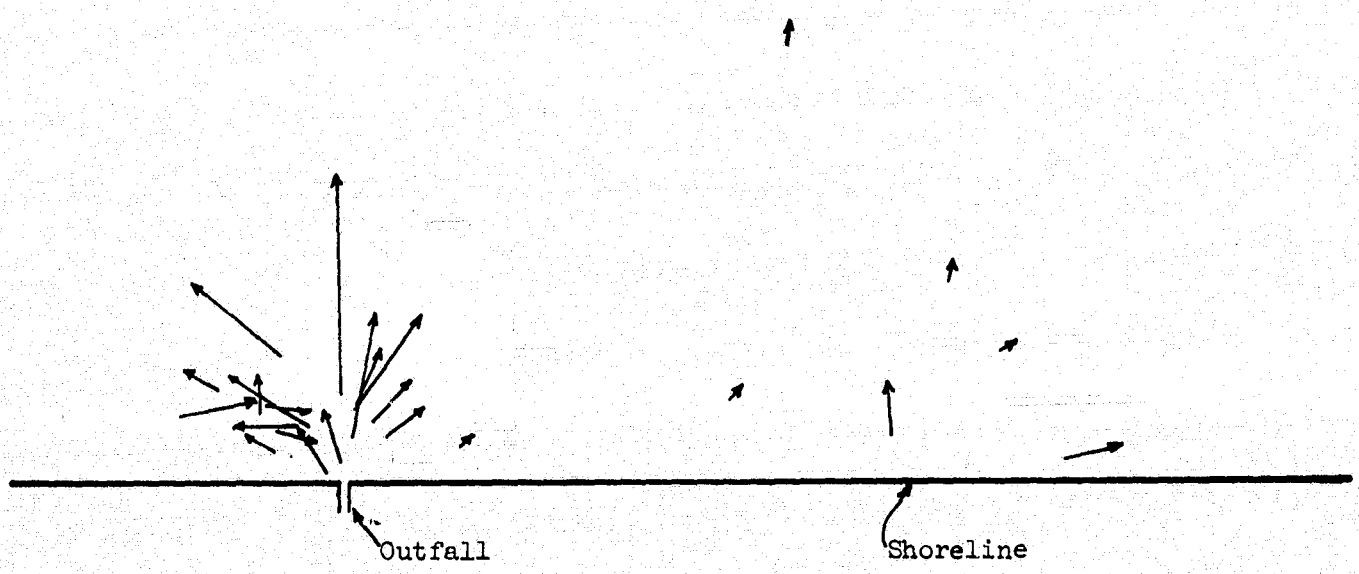

Fig. 19 Horizontal Distribution of Surface Velocities near Outfall

COMPARISON OF FIELD RESULTS WITH MATHEMATICAL MODELS AND LABORATORY OBSERVATIONS

To date there have been no studies, theoretical or experimental, dealing with a submerged buoyant jet discharging horizontally at the shoreline into a finite depth cross flow. It would be possible to extend Fan's (4) model for a buoyant, submerged discharge in a cross flow to three dimensions (i.e., buoyancy in the vertical direction and a jet discharge and cross flow in the horizontal direction) including the effects of finite boundaries (Hirst (6) has dealt with this problem for an infinite fluid (i.e., without boundaries)), or to apply Stolzenback and Harleman's (13), Stefan's (12) or Prych's (10) approach for a surface, shoreline discharge to a submerged, shoreline discharge, including bottom and surface boundaries and a cross flow. In this report, however, extensions of the above models to a submerged, shoreline, buoyant discharge into a finite depth cross flow will not be pursued; such mathematical modelling will be the subject of a later report. The observations from the field survey are compared, however, with some results for a simple, three-dimensional, momentum jet, with some laboratory observations and with some results from the above-mentioned mathematical models for the region after the discharge has reached the river surface in order to aid in the interpretation of the effluent discharge mixing and spreading patterns.

The trajectory of a buoyant submerged jet discharging into a quiescent fluid has been studied mathematically by Abraham (1) and experimentally by Frankel, et. al. (5) and

Rawn (11). The depth of submergence of the outfall in their studies, however, was much greater than in the present study; thus now direct comparison of results can be made. The studies of Fan (4) on a round buoyant jet discharging into a quiescent fluid were not conducted with variables in a range comparable to the present study. The laboratory work of Jen (7), Tamai (14) and Dornhelm (3) dealt with buoyant, surface jets discharging into a quiescent ambient fluid; their results may be comparable to the present study for the the region after the jet has reached the surface, provided the river velocity has little effect on mixing. Experimental results from Pratte and Baines (9) on jet trajectory in a cross flow and from Albertson, et. al. (2) on centerline concentration decrease in a simple jet will also be compared with the results of the present study. Finally, the field observations will be compared with mathematical model predictions of Stolzenback and Harleman (13) and Stefan (12).

A. Variation of Centerline Surface Temperature

Fig. 20 shows the surface temperature concentration decay with distance from the outfall along the centerline of the effluent discharge. The rate of decrease of the surface temperature concentration is very slow for the first 40 - 50 feet from the outfall. Beyond about 60 feet from the outfall the rate of change of the concentration increases and follows the relation

$$\frac{c_m}{c_o} = 6.5 \ (s/D)^{-0.9} \qquad (14)$$

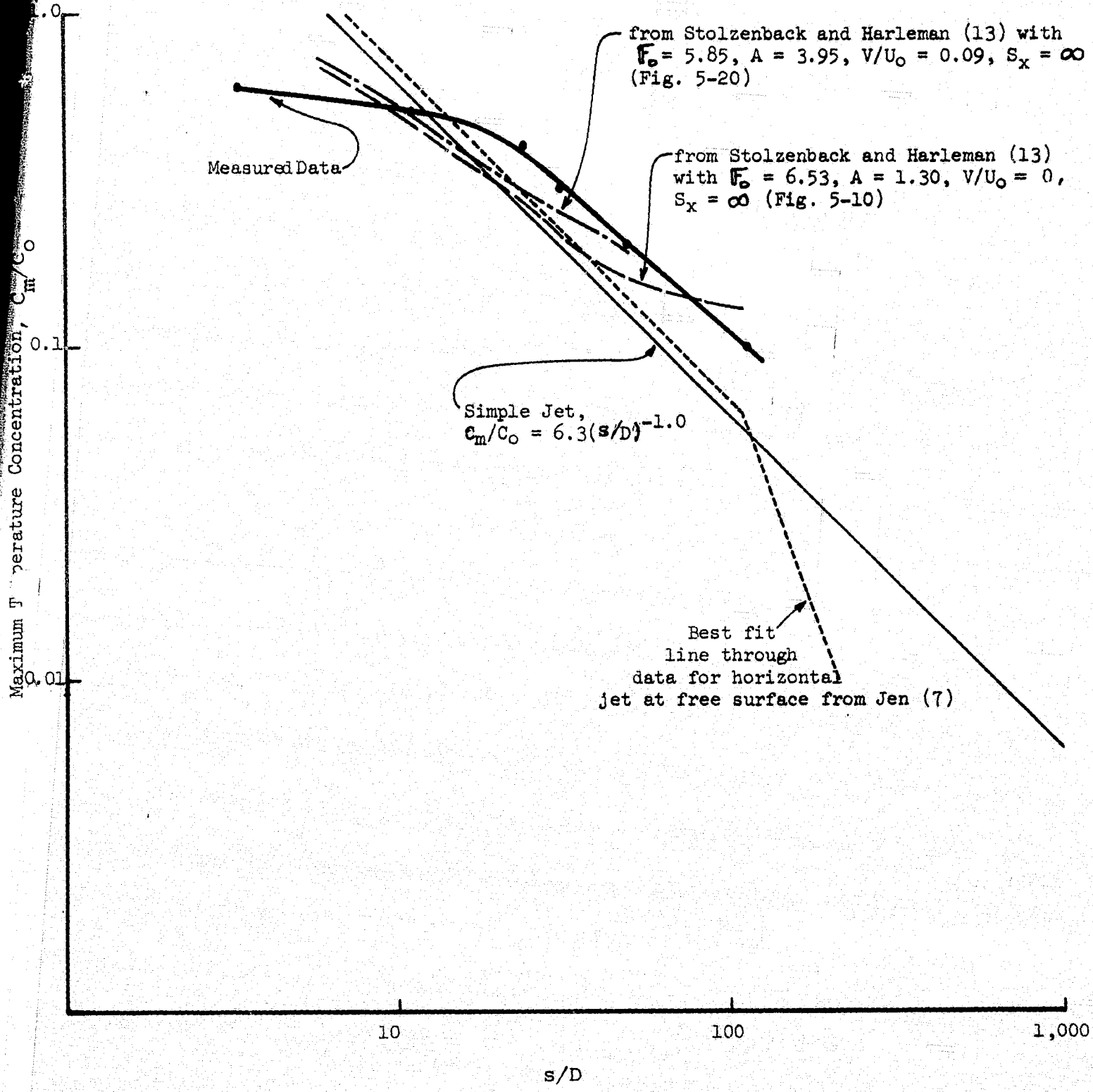

Fig. 20 Surface Temperature Concentration Variation along Effluent Discharge Axis

Also shown in Fig. 20 are results for a simple non-buoyant jet discharging into a quiescent ambient (2), Jen's (7) experimental curve, and two results from Stolzenback and Harleman's model (13) of a buoyant, surface jet discharge. The Stolzenback and Harleman model results (13) in Fig. 20 are for conditions close to those of the field observations (i.e., F_o = 6.0, A = 2.0, V_r/u_o = 0.08, S_x = 1/30); though, as noted previously, their model was developed for a surface discharge.

From Fig. 20, it can be seen that beyond about 50 feet from the outfall the field observations show larger temperature concentrations and a slower rate of temperature decrease, $c_m \sim (s/D)^{-0.9}$, than for a simple, non-buoyant jet (2) and for Jen's (7) experiments where $c_m \sim (s/D)^{-1}$. This difference indicates less total mixing of the effluent discharge with the river than would occur for a simple jet (2) or Jen's (7) buoyant surface jet and results, as discussed in part C of this section, from shoreline and bottom boundaries which reduce the entrainment of river water by the discharge (there were no boundary effects in Jen's work (7)). The Stolzenback and Harleman (13) model predicts a slower rate of temperature decrease except near the outfall than shown by the observations, and the magnitude of the concentrations are higher close to the outfall and lower farther from the outfall than the field measurements. The finite bottom slope and shallow depths near the outfall will result in lower rates of entrainment of river water in this region and could lead to the differences between the model predictions and the observations. The Stolzenback and Harleman model predictions (13) which include the effects of a cross flow (river velocity) tend toward the field observations

with increasing distance from the outfall. For F_o, s/D, outfall shape and wind conditions comparable to the field conditions in this study, Stefan's model (12) predicted temperature concentrations 50-100% greater than the observations and a rate of decay about 1/3 less than the field measurements for the region s/D > 25 (the rate of temperature decrease is very rapid for s/D < 25). Consequently, Stefan's results (12) were not plotted in Fig. 20.

B. Trajectory of Discharge Centerline

The trajectory of the effluent discharge centerline (axis) is shown in Fig. 21. The field observations show that the axis of the effluent discharge is directed slightly upstream for the first 100 feet from the outfall and then is deflected downstream beyond this point. The upstream deflection of the centerline is probably due to the surface shear stress from the strong wind (10-15 mph) blowing upstream; the downstream bending of the centerline results from the deflecting force of the river currents. The downstream deflection of the centerline is affected by the earth fill downstream of the outfall (see Fig. 2) which causes most of the river flow near the outfall to bend to the south (nearly perpendicular to the outfall). This deflection of the river currents results in the effluent discharge being directed across the river as shown in Fig. 21.

Also shown in Fig. 21 are the trajectories obtained from Pratte and Baines' work (9) and from Stolzenback and Harleman's model (13) for similar conditions to the field observations. Pratte and Baines (9) experimentally investigated the trajectory of a jet discharging into a cross flow (i.e., flow perpendicular to the axis of the jet discharge); the effects of buoyancy,

Fig. 21 Trajectory of Effluent Discharge Axis, Comparison with Pratte (9) and Stolzenback and Harleman (13)

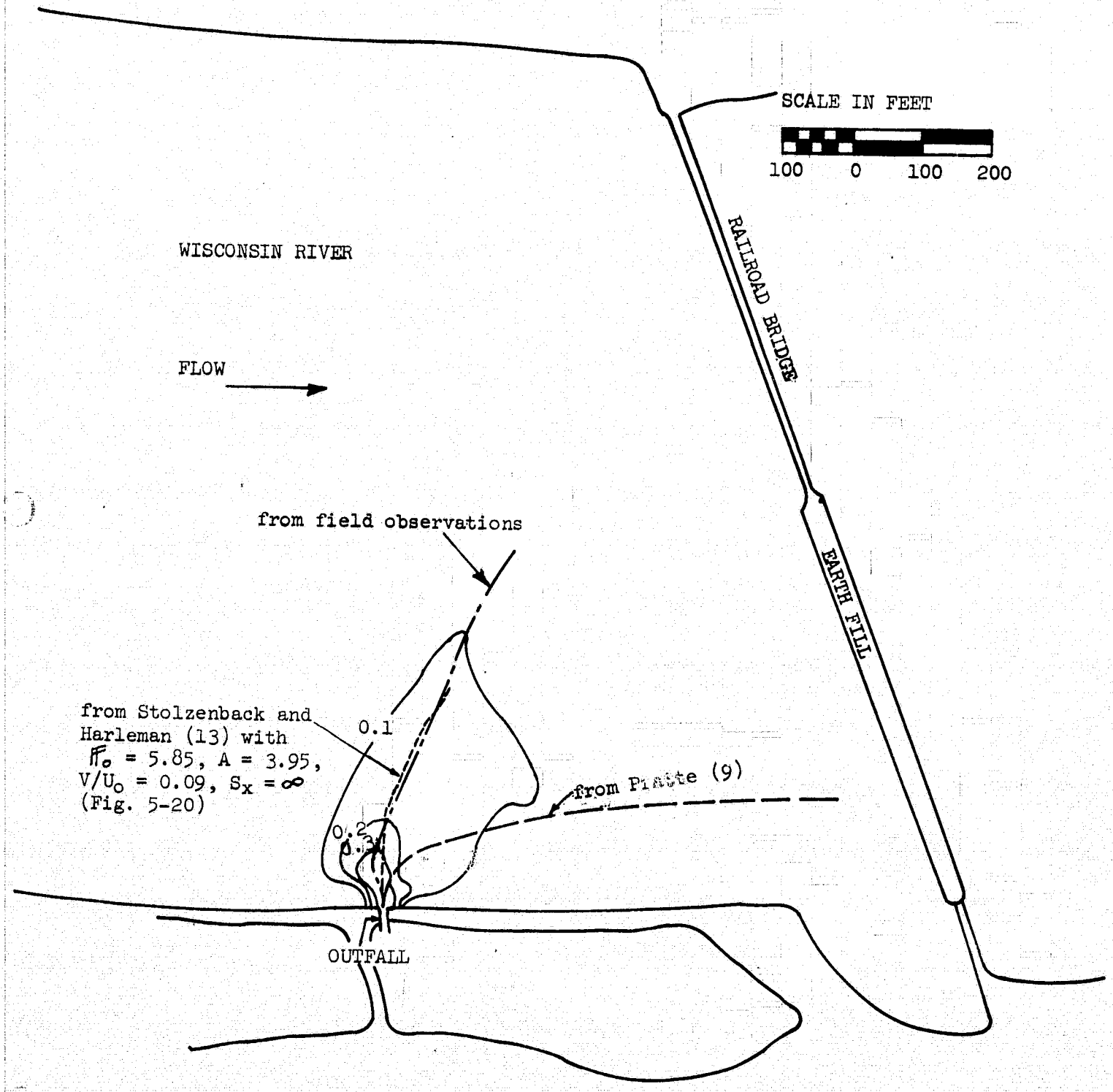

boundaries and cross flow non-uniformity on the trajectory were not studied. In the present study, the effluent discharge is lighter than the river, the water surface and bottom boundaries retard the rate of effluent mixing and the river currents are not uniform in the vicinity of the outfall. Consequently, the results from Pratte and Baines' work (9) are in poor agreement with the field observations except for the first 50 feet from the outfall where the momentum of the effluent discharge governs the mixing. The predicted trajectory from the Stolzenback and Harleman model (13), which is based upon a buoyant, surface discharge into a non-uniform cross flow (namely, a sinusoidal type variation in ambient velocity perpendicular to shore), is in very good agreement with the field observations. Both the Stolzenback and Harleman model results (13) and the field observations indicate that up to about 100 feet from the outfall the river currents have little effect on the effluent discharge trajectory (i.e., the discharge momentum and buoyancy and the river depths govern the trajectory); beyond this point the momentum of the river currents causes the discharge axis to bend downstream. The Stolzenback and Harleman model computations (13) were terminated at a point (about 280 feet from the outfall) where the centerline velocity of the effluent discharge was equal to the component of the river velocity parallel to the centerline of the discharge.

To predict the effluent discharge trajectory beyond the point where the centerline velocities are greater than the river

velocities (i.e., beyond about 280 feet from the outfall), the pattern of river currents is needed. As the velocity measurements were not sufficiently detailed to describe the pattern of river currents (see Fig. 19), a simplified model for the distribution of river velocities was developed. This model is based upon the following assumptions: (1) the flow is steady, two-dimensional and potential; (2) the shorelines and earth fill are approximated by the dashed lines shown in Fig. 22; (3) the flow between the shoreline and the northern end of the earth fill is zero; (4) the effluent discharge does not affect the river flow pattern; and (5) the river flow is uniform 1500 feet upstream from the railroad bridge and earth fill. The streamline pattern for the river flow, obtained by solving La place's equation subject to the above assumptions, is given in Fig. 22. The constant on each streamline in Fig. 22 is the percent of the total river flow passing between the southeast shoreline and that streamline. Magnitudes of river currents at any location are given by the increment of river flow between adjacent streamlines divided by the depth and streamline spacing at the location; the current direction at any point is tangent to the streamline through the point.

Velocity measurements from Fig. 19 for the region away from the outfall where the effluent momentum does not affect the river flow (i.e., beyond about 300 feet from the outfall) are shown in Fig. 22. The measured velocity magnitudes are in good agreement with velocity magnitudes calculated from the streamline pattern in Figure 22 (using the method described above); however, the measured flow directions indicate that the influence of the earth fill in deflecting the flow across the

Fig. 22 Trajectory of Effluent Discharge Axis, Comparison with Simple Jet (2) and Stolzenback and Harleman (13) including Effects of River Currents

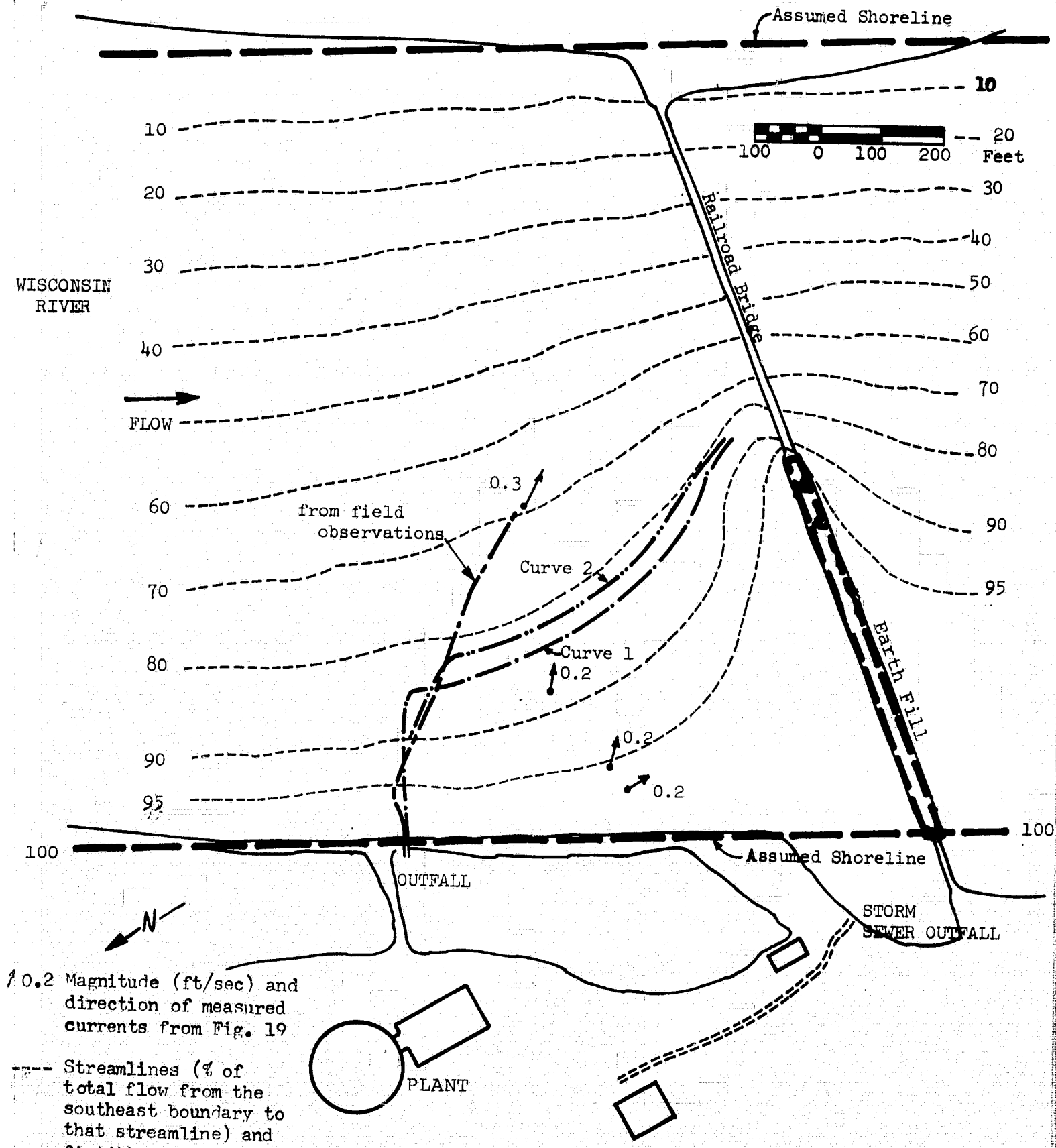

river occurs sooner than predicted in Figure 22. As there are very few measurements (only 4) upon which this comparison is based, it is difficult to determine how representative Figure 22 is of the actual river flow pattern. Nevertheless, the flow pattern in Figure 22 is used, as discussed below, to estimate the effluent discharge centerline for the region where the river velocities govern the trajectory.

Curves 1 and 2 in Figure 22 are predicted effluent discharge trajectories obtained by combining two different models for the region close to the outfall (near field, see Introduction) with the river current pattern in Figure 22 for the region away from the outfall (far field, see Introduction). Curve 1 was obtained by assuming that the discharge penetrated into the river until the centerline velocity of the discharge decreased to the mean river velocity; the river was assumed to be stationary for this initial region. Beyond this point, the discharge was assumed to drift with the river flow so that the discharge centerline follows the river streamline through this point. The centerline velocity of the effluent discharge for the initial or near field region was assumed to be the same as for a simple, three-dimensional, momentum jet and is given by Eq. 4. Curve 2 was obtained using the Stolzenbach and Harleman model (13) result in Figure 21 for the region close to the outfall. At the end of this initial (or near field) region the discharge, as in the case of curve 1, was assumed to drift with

the river flow so that the discharge centerline follows the river streamline through the point at the end of the initial region.

From Fig. 22 it can be seen that curves 1 and 2 are in very poor agreement with the field observations for the far field region (i.e., where the river flow governs the trajectory); through curve 2 (and to a lesser extent curve 1) is in good agreement with the field observations for the initial region. This result strongly suggests (and supports the comments made earlier regarding the comparison of Figs. 19 and 22) that the predicted river current pattern in Fig. 22 does not correspond to the actual river flow pattern. However, it should be noted also that both curves 1 and 2 assume that river currents alone determine the trajectory beyond specific points which mark the end of the near field region (i.e., when the centerline velocity of the discharge is equal to the river velocity or to its component parallel to the centerline of the discharge). Actually there will be a transition zone at the end of the near field region in which the effluent discharge centerline is gradually turned parallel to the river currents. Allowance for this transition zone should improve the agreement between the observed and predicted centerline trajectories. However, as the validity of the predicted river current pattern could not be adequately determined, no attempts have been made to incorporate a transition zone into the predicted trajectories of curves 1 and 2.

C. Lateral and Vertical Spreading of Discharge

Concentration contours from Tamai (14), interpolated from F_o = 3.3 and F_o = 8.4 (F_o = 6.0 in this study), are shown on Figs. 14, 15 and 16. From these figures it can be seen that the concentration contours from the field measurements indicate greater spreading of the effluent discharge, both laterally and vertically, than those from Tamai (14). This increased spreading in the field observations results from the influences of the shoreline and shallow depths near shore ($1.5 < d/D < 3$), the strong wind (10-15 mph) blowing upstream and the outfall submergence. Tamai's work (14) was carried out for a surface discharge into a deep basin ($24 < d/D < 48$) with no shoreline (or back) boundaries and without any wind. Shallow depths and the presence of a shoreline restrict the "free" entrainment of ambient fluid (river water) and result in a rapid initial widening and deepening of the effluent discharge due to reentrainment of the discharge. Away from the shoreline and shallow depths, the lateral and vertical spreading of the effluent discharge will be controlled by the discharge momentum, by the density differences between the effluent and river and by the river momentum and turbulence level. The vertical spreading of the effluent discharge will also be increased (over that observed in Tamai's experiments (14)) due to the vertical mixing resulting from the energy input by the wind.

Fig. 23 shows the lateral surface spread of the effluent discharge with distance from the outfall, where spread is defined as the lateral distance to the point where the concentration is

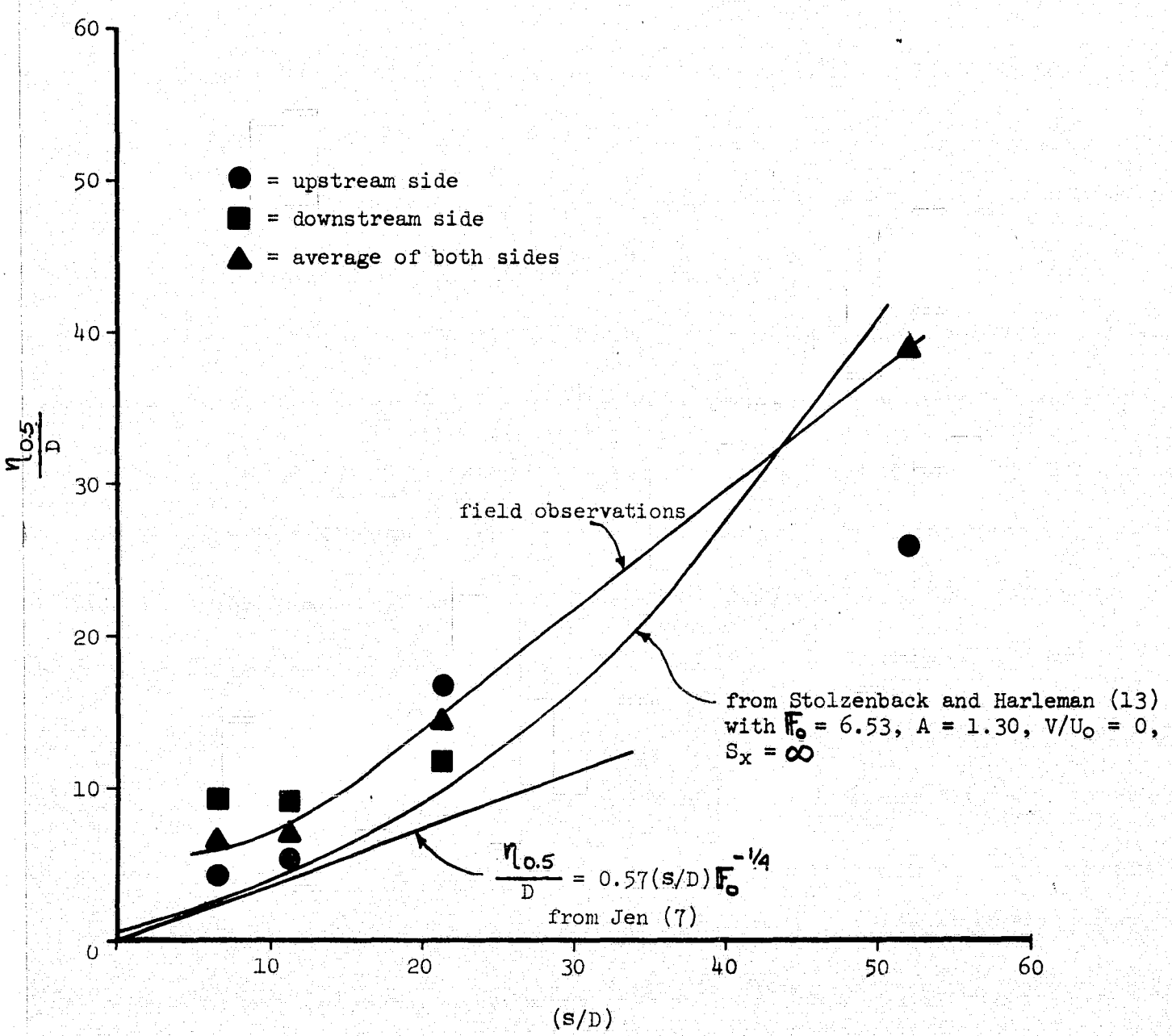

Fig. 23 Comparison of Lateral Surface Spread with Jen (7) and with Stolzenback and Harleman (13)

1/2 of the maximum concentration at that section. From Fig. 23 it can be seen, as noted earlier in Figs. 14-17, that the spread on the upstream side of the effluent discharge (i.e., with respect to an observer looking into the river from the outfall) is about 1/3 to 1/2 smaller than the spread on the downstream side, except for the section at s = 64 feet (s/D = 21.3). At this section (s = 64 feet), the upstream spread is greater than the downstream spread and appears to result from the downstream deflection of the effluent discharge axis which begins very close to this section (see Fig. 7). The greater spreading on the downstream side of the effluent discharge results from the river flow against the discharge. Beyond about 25-30 feet from the outfall (i.e., where the effluent discharge reaches the surface, see Fig. 12), the average spread (i.e., of the upstream and downstream values) increases nearly linearly with distance from the outfall according to the relation

$$\frac{\eta_{0.5}}{D} = 0.85\left(\frac{s}{D}\right) - 2.5 \qquad (15)$$

The experimental result of Jen (7) and the Stolzenback and Harleman model predictions (13) are also plotted in Fig. 23 for comparison with the field observations. Jen's experimental results (7), which were confirmed by Tamai (14) for F_o ranging from 3-11 at large Reynolds numbers ($R_o > 20{,}000$), predict a smaller spread and a slower rate of spread than the field observations. The Stolzenback and Harleman model predictions (13) indicate a smaller spread than the field observations up to about

130 feet from the outfall; beyond this point the Stolzenback and Harleman model predicts a slightly greater spread than the field observations over the range of the measurements. However, the rate of increase of spread close to the outfall (up to about 60 feet from the outfall), predicted by the Stolzenback and Harleman model (13), is in good agreement with the observations. The larger spread of the field observations close to the outfall, compared with the Stolzenback and Harleman model (13) predictions and the results of Jen (7), probably resultsfrom reentrainment of the discharge due to the shallow depths near shore (the Stolzenback and Harleman model predictions shown in Fig. 23 are based upon no bottom effects, $S_x = \infty$).

Lateral surface concentration distributions are plotted in Fig. 24 and compared with Jen's experimental result (7). Both the greater spreading in the field observations, compared with Jen's results (7), and the greater spreading on the downstream side of the discharge, compared with the upstream side, can be seen in Fig. 24. These results were discussed above in connection with Fig. 23. The field observations in Fig. 24 appear to follow a Gaussian distribution for $c/c_m \gtrsim 0.5\text{-}0.6$ but decrease much more slowly than a Gaussian distribution for $c/c_m \lesssim 0.5\text{-}0.6$. Further, the spread of the field observations varies from 40-90% greater than the spread in Jen's results (7). Tamai (14) showed that a Gaussian distribution, with about a 20% greater spread than Jen's result in Fig. 24, described the lateral surface concentration distribution in his experiments for $c/c_m > 0.4$ with $3 < F_o < 11$;

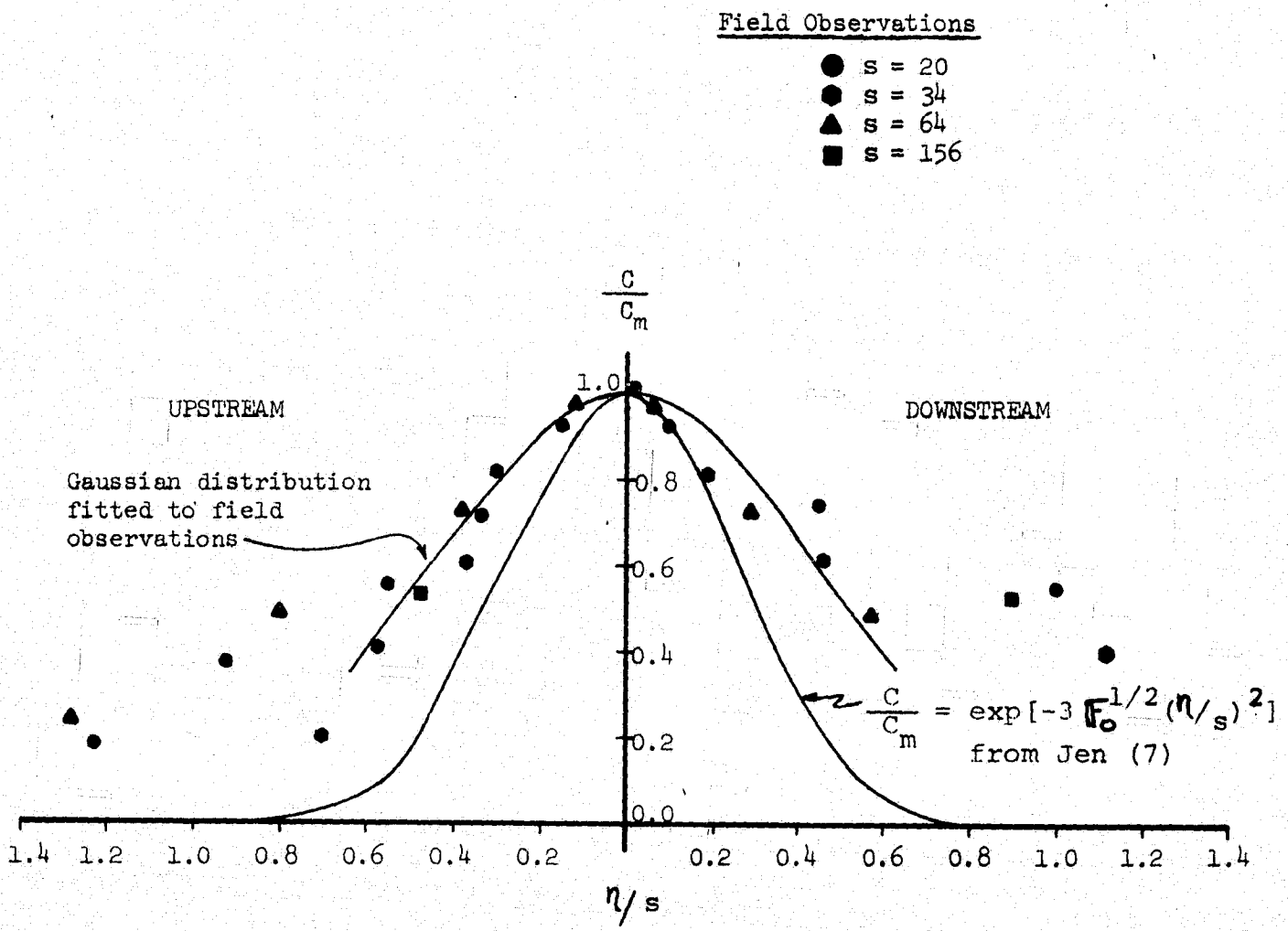

Fig. 24 Lateral Distribution of Surface Temperature Concentration

however, for $c/c_m < 0.4$ the concentration distribution was not Gaussian but decreased more slowly as in the field observations.

Fig. 12 shows the vertical distribution of temperature concentration along the axis of the effluent discharge, based upon the field measurements. Also shown in Fig. 12 is the variation of the vertical spread with distance from the outfall, predicted by the Stolzenback and Harleman model (13), where vertical spread is defined as the depth at which the concentration is 1/2 of the surface concentration at that location. The Stolzenback and Harleman model predictions (13) are in good agreement with the field observations beyond 90-100 feet from the outfall; however, closer to the outfall the model predictions differ significantly from the measurements. The model also predicts that the maximum vertical penetration of the discharge is given by $(0.625D)(0.5\sqrt{F_o}) = 5.63$ feet; the field observations (see Fig. 12) show somewhat greater depths of penetration of the discharge close to the outfall. The differences between the field observations and the model predictions near the outfall appear to be due to the effects of outfall submergence and shallow depths on the entrainment and mixing of the discharge.

EXTENT AND SHAPE OF MIXING ZONE

From the definition presented in the Introduction, the mixing zone is the region bounded by the concentration contour on which

$$c_{mz} = c_o \left(\frac{Q_o}{Q_o+Q_r}\right) , \qquad (16)$$

where c_{mz} = effluent discharge concentration on mixing zone boundary, c_o = effluent discharge concentration at outfall, Q_o = effluent discharge flow rate, Q_r = river flow rate. Using Q_o and Q_r from Table I in Eq. 16 gives $C_{mz}/c_o = 0.007$. The field measurements, however, were not sufficiently extensive to define the longitudinal, lateral or vertical extent of this concentration contour (see sections on presentation and discussion of field observations and comparison of observations with mathematical models and experimental results). Further, measurements were carried out only for the effluent discharge, river and weather conditions of September 12, 1969. Nevertheless, some estimates of the extent and shape of the mixing zone under these conditions may be made by extrapolating the results of the field observations. Moreover, effluent discharge mixing in the region close to the outfall (near field), where outfall discharge conditions affect the spreading and dilution, can be determined from the measurements. Listed below are results regarding the shape and extent of the mixing zone and near field region determined from the field measurements on September 12, 1969:

(1) The longitudinal extent of the mixing zone is approximately 2000 feet from the outfall (i.e., along the centerline of the effluent discharge). This value, which was obtained from the centerline temperature variations in Figure 20 and Eq. 14, must be

regarded as a very rough approximation since the measurements did not extend that far from the outfall and the flow pattern changes markedly beyond about 1000 feet from the outfall where the river discharges underneath the railroad bridge at the earth fill (see Figs. 2 or 22).

(2) Lateral spreading of the effluent discharge is very rapid; measurements up to 150 feet from the outfall indicate a linear increase with distance (see Figure 23) with a total surface width to the concentration contour $c/c_o = 0.1$ of 120 feet (the centerline concentration is $c/c_o = 0.2$). Beyond about 300 feet from the outfall (extent of near field region where outfall discharge conditions affect spreading and dilution), the width of the effluent discharge should increase in proportion to the square root of distance from the outfall due to river turbulence. In addition, the river flow pattern will also affect lateral spreading (i.e., through secondary flows or other flow non-uniformities).

(3) Vertical spreading (i.e., distance to point where the concentration = 1/2 of surface concentration) of the effluent discharge appears to level off in the near field region (up to about 300 feet) at 3-4 feet below the water surface (see Figure 12). However, beyond the near field region due to the wind, the level of river turbulence ($R_r = 2 \times 10^5$ from Table I) and the continuing dilution of the effluent discharge, the effluent is probably partially mixed over the total river depth. As the river temperature profiles indicate a mild stratification (see Figure 4), the effluent discharge concentration would also be expected to exhibit a similar vertical stratification.

(4) The centerline of the mixing zone (and effluent discharge) is determined by the interaction of the effluent discharge with the river currents and with the wind. For the effluent, river and meteorological conditions on the survey the centerline was directed essentially straight outwards from the outfall for about 300 feet into the river; beyond this point the centerline bent gradually downstream in response to the river current pattern.

(5) The extent of the near field region (where outfall discharge conditions affect the spreading and dilution) extends to about 280-300 feet from the outfall (see discussion under part B of previous section). At the end of this region, the maximum effluent concentration (centerline) is $c/c_o = 0.11$ (from Fig. 20). Extrapolating the results from Figure 23 to the end of this region, the total surface width of the discharge to the concentration contour $c/c_o = 0.055$ is 240 feet. Fitting a Gaussian distribution to the results in Figure 24 (though as noted previously a Gaussian curve does not describe the distribution for $c/c_m < 0.5$-0.6), the total surface width of the effluent discharge to $c_{mz}/c_o = 0.007$ would be about 750 feet. Finally, as noted in (3) above, the vertical extent of the mixing zone boundary is probably 3-4 feet below the water surface at the end of the near field region.

As mentioned earlier, these results for the extent and shape of the mixing zone must be regarded as approximate for the field measurements were not sufficiently extensive to define the complete effluent concentration distribution of mixing pattern. In addition, the extent and shape of the mixing zone for effluent, river and weather conditions different from the September 12, 1969, survey must be determined by additional field observations, coupled with mathematical and/or laboratory modelling.

SUMMARY AND CONCLUSIONS

A field survey was conducted on September 12, 1969, of the effluent concentration distributions from the waste water discharge of the Kraft Division Mill, Consolidated Paper Company, into the Wisconsin River at Wisconsin Rapids, Wisconsin. Effluent concentrations were determined from measurements of the temperature distribution; measurements of the velocity distribution in the vicinity of the outfall were also made. Horizontal and vertical concentration patterns of the waste discharge are analyzed and compared with the results of laboratory experiments and of several mathematical models to determine the macroscopic characteristics and relations governing the effluent spreading and dilution for the effluent discharge, river and weather conditions during the survey. These characteristics include the centerline trajectory, the centerline concentration variation, and the lateral and vertical spreads of the effluent discharge. The effects of the shoreline and shallow depths near the outfall, outfall submergence, buoyancy and momentum of the effluent and the pattern and magnitude of river currents on these characteristics are considered. Finally, using the field observations, with results from the laboratory experiments and mathematical models, the extent and shape of the mixing zone is estimated for the particular effluent, river and weather conditions of the survey.

The outfall is submerged and the effluent is buoyant; as a result, the effluent, which is discharged horizontally, bends upward and its centerline intersects the water surface approximately 24 feet from the outfall. The discharge then spreads and mixes rapidly as a surface layer. The trajectory of the effluent

centerline is dominated by the momentum and buoyancy of the effluent over the first 200 - 300 feet from the outfall; beyond this initial region the pattern of river currents governs the trajectory. Beyond the initial submerged region and up to about 300 feet from the outfall, the variation of some of the characteristics of the effluent discharge are reasonably described by the mathematical model of Stolzenback and Harleman (13). However, there are presently available no mathematical models or experimental results which are completely comparable to the effluent discharge and river conditions in this study. Hence there is a need for further research into the spreading and dilution of this type of effluent discharge.

Based on the results from this study the following conclusions may be drawn regarding the spreading and mixing patterns of this waste water discharge:

(1) The submerged effluent discharge becomes a surface layer in a relatively short distance, approximately 24 feet (8 diameters) from the outfall.

(2) The rate of decrease of the surface temperature concentration is very slow for the first 40-50 feet from the outfall (see Fig. 20). Beyond about 60 feet from the outfall the rate of decrease of concentration increases and follows the relation

$$\frac{c_m}{c_o} = 6.5 \left(\frac{s}{D} \right)^{-0.9} . \qquad (14)$$

Equation 14 gives greater concentrations and a slower rate of concentration decrease than for a simple jet which decreases with

distance to the minus 1.0 power. The Stolzenback and Harleman model (13) predicts lower concentrations than the measurements except close to the outfall; the model predictions approach the field observations with increasing distance from the outfall.

(3) Field observations of the trajectory of the effluent discharge centerline are in good agreement with the mathematical model predictions of Stolzenback and Harleman (13) up to about 300 feet from the outfall (see Fig. 21); beyond this point the river currents dominate the effluent centerline trajectory. The extension of the predicted centerline trajectory beyond 300 feet, using a mathematical model of the river current pattern, was in poor agreement with the field measurements (see Fig. 22). The validity of the river current model is not known for insufficient velocity measurements were made; in addition, no allowance (in the extension of the predicted trajectory) was made for a transition zone from an effluent dominated behavior to a river flow dominated behavior.

(4) The average lateral surface spread of the effluent discharge beyond 25-30 feet from the outfall is given by

$$\frac{\eta_{0.5}}{D} = 0.85 \left(\frac{s}{D}\right) - 2.5 \quad . \qquad (15)$$

The variation of the lateral spread with distance from the outfall is similar to that predicted by the Stolzenback and Harleman model (13) (see Fig. 23); however, the observed spread is greater than the predicted spread up to about 130 feet from the outfall.

Beyond this point the predicted spread is greater than the measured spread. The lateral surface concentration distribution appear to follow a Gaussian distribution for $\frac{c}{c_m} > \sim 0.5 - 0.6$ but decreases more slowly than a Gaussian distribution for $\frac{c}{c_m} < \sim 0.5 - 0.6$ (see Fig. 24).

(5) The vertical spreading of the effluent discharge is much more rapid close to the outfall than predicted by the Stolzenback and Harleman model (13) (see Fig. 12) due to outfall submergence and shallow depths. Beyond about 90 feet from the outfall the model predictions are in good agreement with the observations.

(6) Expressions for and discussion of the size and shape of the mixing zone are given in the previous section.

Finally, it should be noted that the above conclusions apply to the particular effluent discharge, river and outfall conditions of the September 12, 1969, survey. Further field observations, coupled with mathematical and laboratory modelling, are required in order to define the spreading and mixing patterns of this waste water discharge for effluent, river and weather conditions different from those during the September 12, 1969, survey.

APPENDIX I - NOTATION

Symbol	Definition
c	Local concentration
c_m	Maximum concentration at any section
c_{mz}	Concentration at mixing zone boundary
c_o	Effluent concentration at outfall
d	River depth
D	Outfall diameter
$\mathbb{F}_o$	Densimetric Froude Number at the outfall = $\frac{u_o}{\sqrt{g\left(\frac{\rho_o-\rho_r}{\rho_r}\right)D}}$
g	Gravitational constant
Q_o	Outfall discharge rate
Q_r	River flow rate
$\mathbb{R}_o$	Outfall Reynolds number = $\frac{u_o D}{\nu}$
$\mathbb{R}_r$	River Reynolds number = $\frac{V_r d}{\nu}$
s	Distance from outfall along axis of effluent discharge
T	Local temperature
T_r	Undisturbed river temperature
T_o	Outfall temperature
u	Local velocity
u_m	Velocity on effluent discharge axis
u_{me}	Horizontal velocity at end of zone of flow establishment
u_o	Outfall velocity

Symbol	Definition
v_e	Vertical velocity at end of zone of flow establishment
V_r	River velocity
x	Horizontal coordinate along outfall axis
y	Vertical coordinate from outfall axis
z	Vertical distance below water surface
η	Lateral (horizontal)distance from discharge axis to any point
$\eta_{0.5}$	Lateral (horizontal) distance from discharge axis to $c/c_m = 0.5$
ν	Kinematic viscosity
ρ_m	Density on effluent discharge axis
ρ_o	Effluent density at outfall
ρ_r	Density of undisturbed river water

APPENDIX II - REFERENCES

1. Abraham, G., "Horizontal Jets in Stagnant Fluid of Other Density", ASCE, Journal of the Hydraulics Division, HY4, Vol. 91, p. 139, July, 1965.

2. Albertson, M. L., Dai, Y. B., Jensen, R. A., and H. Rouse, "Diffusion of Submerged Jets", Proceedings ASCE, Vol. 74, p. 1157, December, 1948.

3. Dornhelm, R., Nouel, M., and R. L. Wiegel, "Velocity and Temperature in Buoyant Surface Jet", ASCE, Journal of the Power Division, PO1, Vol. 98, p. 29, June, 1972.

4. Fan, L. N., "Turbulent Buoyant Jets into Stratified or Flowing Ambient Fluids", W. M. Keck Laboratory of Hydraulics and Water Resources, Division of Engineering and Applied Science, California Institute of Technology, 1967.

5. Frankel, R. J., and J. D. Cumming, "Turbulent Mixing Phenomena of Ocean Outfalls", ASCE, Journal of the Sanitary Engineering Division, SA2, Vol. 91, p. 33, March, 1965.

6. Hirst, E., "Buoyant Jets with Three-Dimensional Trajectories", ASCE, Journal of the Hydraulics Division, HY11, Vol. 98, p. 1999, November 1972.

7. Jen, Yuan, Wiegel, R. L., and I. Mobarek, "Surface Discharge of Horizontal Warm Water Jet", ASCE, Journal of the Power Division, PO2, Vol. 92, p. 1, April, 1966.

8. Policastro, A. J., and J. V. Tokar, "Heated-Effluent Dispersion in Large Lakes: State-of-the-Art of Analytical Modelling. Part 1. Critique of Model Formulations", Argonne National Laboratory, Center for Environmental Studies ANL/ES-11, Argonne, Illinois, January, 1972.

9. Pratte, B. D., and W. D. Baines, "Profiles of the Round Turbulent Jet in Cross Flow", ASCE, Journal of the Hydraulics Division, HY6, Vol. 93, p. 53, November, 1967.

10. Prych, E. A., "A Warm Water Effluent Analyzed as a Buoyant Surface Jet", Sveriges Meteorologiska Och Hydrologiska Institut, Serie Hydrologi Nr. 21, Stockholm, 1972.

11. Rawn, A. M., Bowerman, F. R., and N. H. Brooks, "Diffusers for Disposal of Sewage in Sea Water", ASCE, Journal of the Sanitary Engineering Division, SA2, Vol. 86, p. 65, March, 1960.

12. Stefan, H., Hayakawa, N., and F. R. Schiebe, "Surface Discharge of Heated Water", St. Anthony Falls Hydraulics Laboratory, Technical Report, University of Minnesota, December, 1971.

13. Stolzenbach, K. D., and D. R. F. Harleman, "An Analytical and Experimental Investigation of Surface Discharges of Heated Water", Ralph M. Parsons Laboratory for Water Resources and Hydrodynamics, Technical Report, Massachusetts Institute of Technology, February, 1971.

14. Tamai, N., Wiegel, R. L., and G. F. Tornberg, "Horizontal Surface Discharge of Warm Water Jets", ASCE, Journal of the Power Division, PO2, Vol. 95, p. 253, October, 1969.